Mitochondria-targeting cyclometallated rhodium(III) complexes appended with two rhodamine units as Type I photosensitisers for bioimaging and photocytotoxicity applications by inducing pyroptosis

Katherine Gui-Min Jiang,[ab] Guang-Xi Xu,[a] Lawrence Cho-Cheung Lee,[a] Fangfang Wei,[b] Siye Wu,[b] Keith Man-Chung Wong*[b] and Kenneth Kam-Wing Lo*[ac]

[a] Department of Chemistry, City University of Hong Kong, Tat Chee Avenue, Kowloon, Hong Kong, P. R. China; Email: bhkenlo@cityu.edu.hk

[b] Department of Chemistry, Southern University of Science and Technology, 1088 Xueyuan Boulevard, Shenzhen 518055, P. R. China; Email: keithwongmc@sustech.edu.cn

[c] State Key Laboratory of Terahertz and Millimetre Waves, City University of Hong Kong, Tat Chee Avenue, Kowloon, Hong Kong, P. R. China

Supplementary Information

Table of Contents Pages

Experimental Section

Materials and reagents

All solvents were of analytical reagent grade and purified according to standard procedures.[1] Rose Bengal and 1,3-diphenylisobenzofuran (DPBF) were purchased from Acros. Benzil, 1,2-benzenediamine, chloranil, selenium dioxide and 2,3-diaminonaphthalene were purchased from Aladdin. Acetic acid, 3-(diethylamino)phenol, 2',7'-dichlorodihydrofluorescin diacetate (DCFH-DA), 2,3-phenylquinoxaline (Hdpqx), $RhCl_3 \bullet nH_2O$ and bovine serum albumin (BSA) were purchased from Sigma-Aldrich. 4,4'-Dimethyl-2,2'-bipyridine (Me_2-bpy), 2,2'-thenil, NH_4PF_6 and rhodamine 123 (R123) were purchased from Bide. 5,5-Dimethyl-1-pyrroline *N*-oxide (DMPO), 3-(4,5-dimethylthiazol-2-yl)-2,5-diphenyltetrazolium bromide (MTT), Na_2CO_3, NaOH, $Na_2S_2O_5$, $MgSO_4$ and *p*-toluenesulfonic acid were purchased from Energy Chemical Company. Dihydrorhodamine 123 (DHR123), Ferrostatin-1 (Fer-1), z-VAD-fmk, Necrostatin-1 (Ner-1) and necrosulfonamide (NSA) were purchased from MedChemExpress. Hydroxylphenyl fluorescein (HPF) was purchased from MKbio. All these chemicals were used without further purification. 2,2'-Bipyridine-4,4'-dicarboxaldehyde (bpy-diCHO),[2] 2,3-di(thiophen-2-yl)quinoxaline (Hdtqx), 2,3-diphenylbenzo[*g*]quinoxaline (Hdpbq), 2,3-di(thiophen-2-yl)benzo[*g*]quinoxaline (Hdtbq)[3] and the rhodium(III) chloro-bridged dimers $[Rh_2(N\hat{}C)_4Cl_2]$ (HN^C = Hdpqx, Hdtqx, Hdpbq and Hdtbq)[4] were prepared according to modified procedures. All buffer components were of biological grade and used as received. Autoclaved Milli-Q water was used for the preparation of the aqueous solutions. Dulbecco's modified Eagle's medium (DMEM), fetal bovine serum (FBS), phosphate-buffered saline (PBS), trypsin-EDTA (0.25%, with phenol red) and penicillin/streptomycin were purchased from Gibco. MitoTracker Green, Calcein-AM,

propidium iodide (PI), Alexa Fluor 488-labeled goat anti-rabbit IgG(H+L), Hoechst 33258, BCA protein assay kit and prestained colour protein molecular weight marker were purchased from Beyotime. MitoTracker Deep Red, lactate dehydrogenase (LDH) cytotoxicity assay kit and secondary antibody lgG(H+L)/HRP were purchased from Invitrogen. RIPA lysis buffer, primary antibodies of caspase-1, β-actin and GAPDH were obtained from Solarbio. Primary antibody of gasdermin D (GSDMD) was purchased from Huabio. MCF-7 cells were obtained from the American Type Culture Collection. The growth medium for cell culture contained DMEM with 10% FBS and 1% penicillin/streptomycin.

Synthesis and Characterisation

(bpy-diRho)(PF$_6$)$_2$

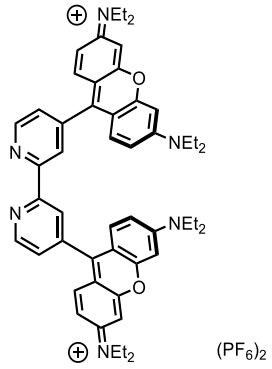

A mixture of bpy-diCHO (100 mg, 0.5 mmol), 3-(diethylamino)phenol (330 mg, 2 mmol), *p*-toluenesulfonic acid (9 mg, 0.05 mmol) and acetic acid (100 mL) was heated to 100°C and stirred for 12 h. The mixture was neutralised by NaOH and the precipitate was filtered and dissolved in CH_2Cl_2 (100 mL). The solvent was dried over anhydrous $MgSO_4$ and filtered. Chloranil (12 mg, 0.05 mmol) was added to the filtrate, and the mixture was stirred at room temperature for 2 h. The solvent was removed under reduced pressure to yield a purple solid, which was subsequently dissolved in CH_3CN (50 mL). The solution was further stirred for 1 h after the addition of solid NH_4PF_6 (815 mg, 5 mmol). The solvent was removed by rotary evaporation to give a purple solid, which was further purified by column chromatography on silica gel using CH_2Cl_2/CH_3CN (30:1, *v/v*) as the eluent. Subsequent recrystallisation of the solid from CH_2Cl_2/Et_2O afforded (bpy-diRho)(PF$_6$)$_2$ as purple crystals. Yield: 340 mg (62%). ^{1}H NMR (400 MHz, CD_3CN, 298 K, TMS): δ8.89 (d, J = 4.9 Hz, 2H, H6 and H6' of bpy), 8.56 (s, 2H, H3 and H3' of bpy), 7.51 (d, J = 4.9 and 1.6 Hz, 2H, H5 and H5' of bpy), 7.34 (d, J = 9.6 Hz, 4H, H1 and H8 of xanthene), 7.00 (dd, J = 9.4 and 2.5 Hz, 4H, H2 and H7 of xanthene), 6.89 (d, J = 2.4 Hz, 4H, H4 and H6 of xanthene), 3.65 (q, J = 7.2 Hz, 16H, CH_2CH$_3$), 1.28 (t, J = 7.1 Hz, 24H, CH$_2$CH_3). ^{13}C NMR (150 MHz, CD_3CN, 298 K, TMS): δ158.51, 156.38, 150.59, 131.89, 125.06, 121.43, 115.12, 113.27, 96.79,

46.41, 12.46. Elemental analysis (%) calcd for $C_{52}H_{58}N_6O_2P_2F_{12}\cdot CH_2Cl_2$: C 54.23, H 5.15, N 7.16, found: C 54.07, H 5.28, N 7.23.

[Rh(dpqx)$_2$(bpy-diRho)](PF$_6$)$_3$ ***(1)***

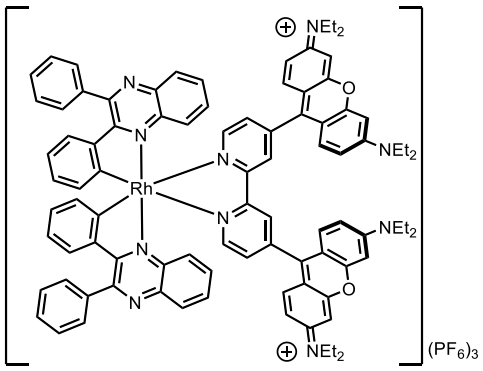

A mixture of [Rh$_2$(dpqx)$_4$Cl$_2$] (70 mg, 0.05 mmol) and (bpy-diRho)(PF$_6$)$_2$ (110 mg, 0.1 mmol) in CH_2Cl_2/MeOH (50 mL) (1:1, *v/v*) was stirred in the dark at room temperature for 2 h. The mixture was further stirred for 1 h after the addition of solid NH_4PF_6 (82 mg, 0.5 mmol). The solvent was removed under reduced pressure and the purple residual solid was purified by column chromatography on silica gel using CH_2Cl_2/CH_3CN (20:1, *v/v*) as the eluent. The solvent was removed under reduced pressure to give a purple solid. Subsequent recrystallisation of the solid from CH_2Cl_2/Et_2O afforded the complex as purple crystals. Yield: 66 mg (70%). ^{1}H NMR (400 MHz, CD_3CN, 298 K, TMS): δ 9.24 (d, J = 5.5 Hz, 2H, H6 and H6' of bpy), 8.11 (dd, J = 8.3 and 1.0 Hz, 2H, H5 of quinoxaline of dpqx), 8.00 (s, 2H, H3 and H3' of bpy), 7.99 – 7.95 (m, 4H, H2 and H6 of 3-phenyl ring of dpqx), 7.90 (dd, J = 5.5 and 1.5 Hz, 2H, H5 and H5' of bpy), 7.86 – 7.77 (m, 4H, H6 and H8 of quinoxaline of dpqx), 7.75 – 7.68 (m, 6H, H3, H4 and H5 of 3-phenyl ring of dpqx), 7.54 – 7.48 (m, 2H, H7 of quinoxaline of dpqx), 7.31 (dd, J = 8.0 and 1.5 Hz, 2H, H3 of 2-phenyl ring of dpqx), 7.11 (d, J = 9.6 Hz, 2H, H1 of xanthene of bpy-diRho), 6.98 (dd, J = 9.6 and 2.4 Hz, 2H, H2 of xanthene of bpy-diRho), 6.93 – 6.80 (m, 6H, H4 and H5 of 2-phenyl ring of dpqx and H4 of xanthene), 6.77 (d, J = 2.4 Hz, 2H, H5 of xanthene of bpy-diRho), 6.74 (dd, J = 9.6 and 2.4 Hz, 2H, H6 of 3-phenyl ring of dpqx), 6.63 (dd, J = 9.6 and 2.4 Hz, 2H, H7 of xanthene of bpy-diRho), 6.50 (d, J = 9.6 Hz, 2H, H8 of xanthene of bpy-

diRho), 3.68 – 3.53 (m, 16 H, C*H*$_2$CH$_3$), 1.27 – 1.16 (m, 24 H, CH$_2$C*H*$_3$). ^{13}C NMR (150 MHz, CD$_3$CN, 298 K, TMS): δ 158.31, 158.21, 156.48, 156.27, 155.16, 150.88, 150.34, 145.16, 145.09, 143.14, 141.47, 140.33, 140.17, 139.97, 136.58, 132.12, 131.65, 131.39, 131.15, 130.91, 130.55, 129.86, 129.78, 129.43, 125.43, 125.16, 124.58, 124.15, 115.34, 114.87, 112.81, 97.03, 96.91, 46.45, 12.39. HR-ESI-MS calcd for RhC$_{92}$H$_{84}$N$_{10}$O$_2$P$_2$F$_{12}$ ([M – PF$_6$]$^+$): *m*/*z* 1753.51119, found: 1753.50768. Elemental analysis (%) calcd for RhC$_{92}$H$_{84}$N$_{10}$O$_2$P$_3$F$_{18}$·2H$_2$O: C 57.09, H 4.58, N 7.24, found: C 56.91, H 4.47, N 7.13.

[Rh(dtqx)$_2$(bpy-diRho)](PF$_6$)$_3$ (***2***)

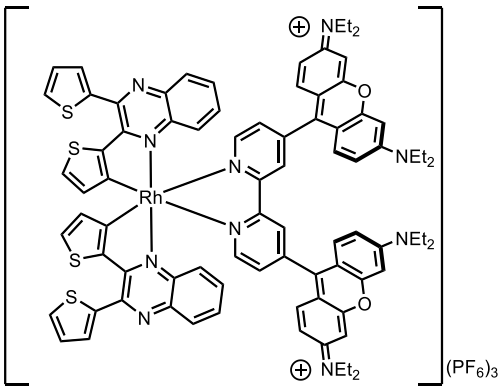

The synthetic procedure was similar to that for complex **1**, except [Rh$_2$(dtqx)$_4$Cl$_2$] (72 mg, 0.05 mmol) was used instead of [Rh$_2$(dpqx)$_4$Cl$_2$]. The solvent was removed under reduced pressure and the purple residual solid was purified by column chromatography on silica gel using CH_2Cl_2/CH_3CN (20:1, *v/v*) as the eluent. The solvent was removed under reduced pressure to give a purple solid. Subsequent recrystallisation of the solid from CH_2Cl_2/Et_2O afforded the complex as purple crystals. Yield: 56 mg (58%). ^{1}H NMR (400 MHz, CD_3CN, 298 K, TMS): δ 8.76 (d, J = 5.5 Hz, 2H, H6 and H6' of bpy), 8.13 (s, 2H, H3 and H3' of bpy), 8.08 (d, J = 8.3 Hz, 2H, H5 of quinoxaline of dtqx), 7.91 – 7.85 (m, 4H, H3 and H5 of 3-thienyl ring of dtqx), 7.81 – 7.73 (m, 4H, H5 and H5' of bpy and H6 of quinoxaline of dtqx), 7.55 (d, J = 5.0 Hz, 2H, H5 of 2-thienyl ring of dtqx), 7.52 – 7.46 (m, 4H, H8 of quinoxaline and H4 of 3-thienyl ring of dtqx), 7.35 (dd, J = 4.8 and 3.7 Hz, 2H, H7 of quinoxaline of dtqx), 7.18 (d, J = 9.6 Hz, 2H, H1 of xanthene of bpy-diRho), 7.01 (dd, J = 9.6 and 2.4 Hz, 2H, H2 of xanthene of bpy-diRho), 6.83 (d, J = 2.3 Hz, 2H, H4 of xanthene of bpy-diRho), 6.80 (d, J = 2.3 Hz, 2H, H5 of xanthene of bpy-diRho), 6.77 (dd, J = 9.5 and 2.4 Hz, 2H, H7 of xanthene of bpy-diRho), 6.52 (d, J = 5.0 Hz, 2H, H4 of 2-thienyl ring of dtqx), 6.48 (d, J = 9.5 Hz, H8 of xanthene of bpy-diRho), 3.69 – 3.56 (m, 16H, CH_2CH$_3$), 1.28 – 1.20 (m, 24 H, CH$_2$CH_3). ^{13}C NMR (150 MHz, CD_3CN, 298 K, TMS): δ 157.46, 156.49, 156.26,

155.40, 150.87, 150.49, 147.76, 145.17, 140.94, 140.50, 138.24, 137.59, 134.44, 133.23, 132.48, 131.95, 131.48, 130.98, 130.71, 130.28, 129.56, 128.15, 125.37, 123.95, 115.38, 114.92, 112.82, 112.80, 96.99, 96.94, 46.45, 30.68, 12.37. HR-ESI-MS calcd for $RhC_{84}H_{76}N_{10}O_2S_4P_2F_{12}$ ($[M - PF_6]^+$): *m/z* 1777.33687, found: 1777.33577. Elemental analysis (%) calcd for $RhC_{84}H_{76}N_{10}O_2S_4P_3F_{18}\cdot H_2O$: C, 51.96, H, 4.05, N, 7.21, found: C, 51.92, H, 4.05, N, 7.13.

[Rh(dpbq)$_2$(bpy-diRho)](PF$_6$)$_3$ ***(3)***

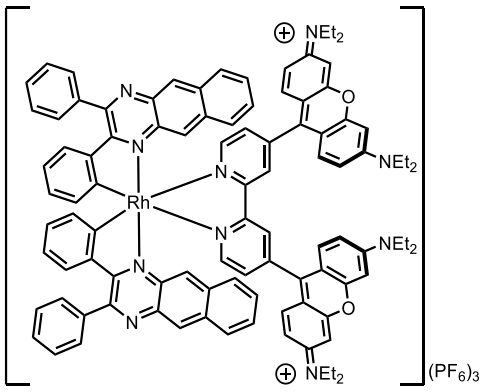

The synthetic procedure was similar to that for complex **1**, except [Rh$_2$(dpbq)$_4$Cl$_2$] (80 mg, 0.05 mmol) was used instead of [Rh$_2$(dpqx)$_4$Cl$_2$]. The solvent was removed under reduced pressure and the purple residual solid was purified by column chromatography on silica gel using CH$_2$Cl$_2$/CH$_3$CN (20:1, *v/v*) as the eluent. The solvent was removed under reduced pressure to give a purple solid. Subsequent recrystallisation of the solid from CH$_2$Cl$_2$/Et$_2$O afforded the complex as purple crystals. Yield: 66 mg (66%). ^{1}H NMR (600 MHz, CD$_3$CN, 298 K, TMS): δ9.59 (d, J = 5.5 Hz, 2H, H6 and H6' of bpy), 8.77 (s, 2H, H5 of benzo[*g*]quinoxaline of dpbq), 8.43 (s, 2H, H10 of benzo[*g*]quinoxaline of dpbq), 8.21 (d, J = 8.5 Hz, 2H, H9 of benzo[*g*]quinoxaline of dpbq), 8.13 – 8.09 (m, 4H, H2 and H6 of 3-phenyl ring of dpbq), 8.04 (d, J = 5.6 Hz, 2H, H5 and H5' of bpy), 7.88 (s, 2H, H3 and H3' of bpy), 7.78 – 7.73 (m, 6H, H3, H4 and H5 of 3-phenyl ring of dpbq), 7.68 – 7.63 (m, H6 and H7 of benzo[*g*]quinoxaline of dpbq), 7.56 – 7.51 (m, 2H, H8 of benzo[*g*]quinoxaline of dpbq), 7.39 (d, J = 7.9 Hz, 2H, H6 of 2-phenyl ring of dpbq), 6.94 – 6.90 (m, 2H, H5 of 2-phenyl ring of dpbq), 6.86 – 6.80 (m, 4H, H4 of 2-phenyl ring of dpbq and H2 of xanthene of bpy-diRho), 6.76 (d, J = 2.3 Hz, 2H, H4 of xanthene of bpy-diRho), 6.74 (s, 2H, H1 of xanthene of bpy-diRho), 6.62 (d, J = 9.5 Hz, 2H, H8 of xanthene of bpy-diRho), 6.58 (s, 4H, H3 of 2-phenyl ring and H5 of xanthene of bpy-diRho), 6.42 (dd, J = 9.6 and 2.3 Hz, 2H, H7 of xanthene of bpy-diRho), 3.60 – 3.51 (m, 16H, C*H*$_2$CH$_3$), 1.23 – 1.16 (m, 24H,

CH_2CH_3). ^{13}C NMR (150 MHz, CD_3CN, 298 K, TMS): δ 171.03 ($J_{C–Rh}$ = 31.0 Hz), 161.79, 158.18, 156.30, 156.19, 155.39, 155.36, 150.90, 150.65, 145.67, 145.24, 140.30, 138.16, 137.00, 136.91, 134.46, 134.12, 132.77, 131.32, 131.29, 131.18, 130.96, 130.01, 129.79, 129.30, 129.11, 129.08, 128.32, 125.40, 124.17, 123.74, 114.85, 114.80, 112.85, 112.65, 96.91, 96.87, 54.91, 46.44, 12.38. HR-ESI-MS calcd for $RhC_{100}H_{88}N_{10}O_2P_2F_{12}$ ($[M – PF_6]^+$) *m*/*z*: 1853.54224; found: 1853.54249. Elemental analysis (%) calcd for $RhC_{100}H_{88}N_{10}O_2P_3F_{18}\cdot 2H_2O$: C 59.00, H 4.56, N 6.88, found: C 58.74, H 4.50, N 6.75.

[Rh(dtbq)$_2$(bpy-diRho)](PF$_6$)$_3$ (***4***)

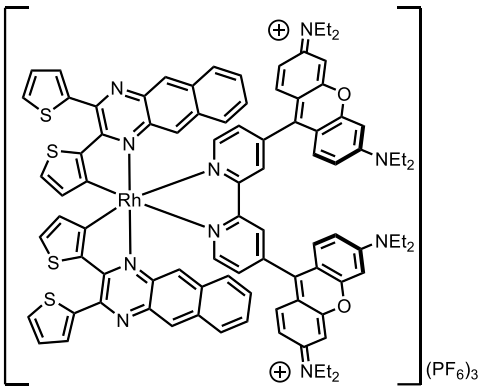

The synthetic procedure was similar to that for complex **1**, except [Rh$_2$(dtbq)$_4$Cl$_2$] (82 mg, 0.05 mmol) was used instead of [Rh$_2$(dpqx)$_4$Cl$_2$]. The solvent was removed under reduced pressure and the purple residual solid was purified by column chromatography on silica gel using CH$_2$Cl$_2$/CH$_3$CN (20:1, *v*/*v*) as the eluent. The solvent was removed under reduced pressure to give a purple solid. Subsequent recrystallisation of the solid from CH$_2$Cl$_2$/Et$_2$O afforded the complex as purple crystals. Yield: 61 mg (62%). ^{1}H NMR (600 MHz, CD$_3$CN, 298 K, TMS): δ9.07 (d, J = 5.5 Hz, 2H, H6 and H6' of bpy), 8.63 (s, 2H, H5 of benzo[*g*]quinoxaline of dtbq), 8.09 (d, J = 8.4 Hz, H6 of benzo[*g*]quinoxaline of dtbq), 7.98 – 7.94 (m, 4H, H3 and H3' of bpy and H10 of benzo[*g*]quinoxaline of dtbq), 7.90 (dd, J = 3.6 and 1.1 Hz, H3 of 3-thienyl ring of dtbq), 7.88 – 7.83 (m, 4H, H5 and H5' of bpy and H5 of 3-thienyl ring of dtbq), 7.56 – 7.52 (m, 2H, H7 of benzo[*g*]quinoxaline of dtbq), 7.47 (d, J = 4.9 Hz, 2H, H4 of 2-thienyl ring of dtbq), 7.43 – 7.34 (m, 4H, H8 and H9 of benzo[*g*]quinoxaline of dtbq), 7.30 (dd, 2H, J = 5.1 and 3.6 Hz, H4 of 3-thienyl ring of dtbq), 6.81 (d, J = 9.5 Hz, 2H, H1 of xanthene of bpy-diRho), 6.70 (d, J = 2.4 Hz, 2H, H4 of xanthene of bpy-diRho), 6.68 (d, J = 2.4 Hz, 2H, H5 of xanthene of bpy-diRho), 6.67 – 6.63 (m, 4H, H2 of xanthene of bpy-diRho and H5 of 2-thienyl ring of dtbq), 6.56 (dd, J = 9.6 and 2.4 Hz, 2H, H7 of xanthene of bpy-diRho), 6.49 (d, J = 9.6 Hz, 2H, H8 of xanthene of bpy-diRho), 3.52 – 3.46 (m, 16H, C*H*$_2$CH$_3$), 1.20 (t, J = 6.9 Hz, 24H, CH$_2$C*H*$_3$). ^{13}C NMR (150 MHz,

CD_3CN, 298 K, TMS): δ 158.21, 156.27, 155.54, 150.82, 150.76, 148.74, 145.26, 138.51, 138.42, 137.57, 137.49, 135.59, 134.57 133.84, 133.67, 132.37, 131.53, 131.03, 130.98, 129.54, 129.40, 129.11, 129.03, 128.22, 128.14, 127.93, 125.66, 121.71, 114.94, 114.86, 112.82, 112.68, 96.94, 46.46, 12.38. HR-ESI-MS calcd for $RhC_{92}H_{84}N_{10}O_2S_4P_2F_{12}$ ($[M - PF_6]^+$): *m*/*z* 1877.36817, found: 1877.36743. Elemental analysis (%) calcd for $RhC_{92}H_{80}N_{10}O_2S_4P_3F_{18}\cdot 2H_2O$: C 53.65, H 4.11, N 6.80, found: C 53.77, H 4.05, N 6.66.

Physical Measurements and Instrumentation

^{1}H and ^{13}C NMR spectra were obtained on a Bruker AVANCE III 400 or 600 MHz spectrometre with Prodigy Platform at 298 K using deuterated acetonitrile (CD_3CN). Chemical shifts (δ, ppm) were reported relative to tetramethylsilane (TMS). High-resolution electrospray ionisation (HR-ESI) mass spectra were recorded on a high-energy collision dissociation Q-Exactive Orbitrap Fusion Tribrid mass spectrometer at 298 K. Elemental analyses were carried out on an Elementar Analysensystem GmbH Vario MICRO elemental analyser. Electronic absorption spectra were taken on a Cary 60 UV-vis spectrophotometer. Steady-state emission spectra were recorded on an Edinburgh Instruments FS5 spectrofluorometer. Quartz cuvettes (path length = 1 cm) were used in all spectrophotometric and fluorometric measurements. Emission quantum yields were measured by Hamamatsu-C11347.

X-ray Structural Analysis

Single crystals of the complex suitable for X-ray crystallographic studies were obtained by slow diffusion of Et_2O vapour into CH_2Cl_2 solutions of the complexes. Single crystal X-ray data were collected on a Single Crystal X-ray Diffractometer (Bruker D8 Venture) using Mo $K\alpha$ radiation (λ = 0.71073 Å). Data collection was performed using SAINT V8.38A (Bruker AXS Inc., 2017) programme and refined by the SHELXL2016/6 (Sheldrick, 2016) programme. All e.s.d.'s (except the e.s.d. in the dihedral angle between two least-squares planes) were estimated using full covariance matrix. The corresponding electron density was treated by the PLATON/SQUEEZE procedure and the solvent and counterion molecules were omitted in the final model. The X-ray crystallographic data for complex **1** have been deposited at the Cambridge Crystallographic Data Centre (CCDC), under the deposition number CCDC 2469873.

The data can be obtained free of charge from the CCDC via www.ccdc.cam.ac.uk/data_request/cif.

Transient Absorption (TA) Spectroscopy

Nanosecond time-resolved TA difference spectra were measured on an Edinburgh Instruments LP920 laser flash photolysis spectrometer using the third harmonic output (532 nm; 6 – 8 ns fwhm pulse width) of a Spectra-Physics Quanta-Ray Q-switched LAB-150 pulsed Nd: YAG laser (10 Hz) as the excitation source. Unless specified otherwise, all solutions for transient absorption studies were deaerated on a high-vacuum line in a two-compartment cell consisting of a 10-mL Pyrex bulb and a 1-cm path length quartz cuvette. The cells were sealed from the atmosphere using a Bibby Rotaflo HP6 quick-release Teflon stopper. The solutions were rigorously deaerated with no fewer than four successive freeze-pump-thaw cycles.

Determination of Singlet Oxygen ($^1O_2$) Generation Quantum Yields

The $^1O_2$ generation quantum yields were measured by the optically dilute method[5] using Rose Bengal as the reference (Φ_Δ = 0.45 in aerated CH_3CN).[6] An aerated CH_3CN solution (2 mL) containing the samples was introduced to a quartz cuvette of 1-cm path length. The absorbance of the samples and Rose Bengal was *ca.* 0.4 at λ = 570 nm. The solutions were excited at λ = 570 nm and the emission spectra of $^1O_2$ at 1200 – 1350 nm were recorded. The $^1O_2$ generation quantum yields of the samples were calculated according to the following equation:

$$\Phi_{\Delta s} = \Phi_{\Delta r}\left(\frac{I_r}{I_s}\right)\left(\frac{B_r}{B_s}\right)\left(\frac{n_s}{n_r}\right)^2\left(\frac{D_s}{D_r}\right)$$

where the subscripts *s* and *r* refer to the sample and reference solutions, respectively,

Φ_Δ is $^1O_2$ generation quantum yield, I is excitation intensity, B is $1 - 10^{-AL}$, A is absorbance at the excitation wavelength, L is path length in cm, n is refractive index of the solvent and D is integrated intensity.

The $^1O_2$ generation quantum yields were also determined by monitoring the diminution rate of DPBF absorption at λ = 410 nm in aerated CH_3CN using Rose Bengal as the reference (Φ_Δ = 0.45 in aerated CH_3CN).[6] An aerated CH_3CN solution (2 mL) containing the sample and DPBF was introduced to a quartz cuvette of 1-cm path length and irradiated at λ = 570 nm. The absorbance of DPBF was *ca.* 1.0 at λ = 410 nm and the absorbance of the complex and Rose Bengal was *ca.* 0.4 at λ = 570 nm. The Φ_Δ values of the complexes were determined using the following equation:

$$\Phi_{\Delta s} = \Phi_{\Delta r} \frac{m_s F_r}{m_r F_s}$$

where the subscripts *s* and *r* refer to the sample and reference solutions, respectively, Φ_Δ is $^1O_2$ generation quantum yield, m is the slope of a linear fit of the change in absorption of DPBF at λ_{abs} = 410 nm against the irradiation time and F is the absorption correlation factor, which is given as $F = 1 - 10^{-AL}$ (A = absorbance at λ = 570 nm and L = path length of cuvette).

Cyclic Voltammetry

Cyclic voltammetry studies were conducted on a CH Instrument, Inc., model CHI 600A electrochemical analyser. The experiments were performed in a reservoir with a working volume of 4 mL. A platinum wire served as the counter electrode and was placed in the working electrode compartment. The working and reference electrodes were a glassy carbon electrode and an Ag^+/Ag pseudoreference electrode. The

measurements were conducted in a non-aqueous medium (0.1 M $^{n}Bu_4NPF_6$ in CH_3CN) at 298 K. The ferrocenium/ferrocene ($FeCp_2^{+/0}$) redox couple was used as the internal reference for potential calibration. Prior to each experiment, the glassy carbon working electrode was polished to a mirror-like finish with 0.3 μm α-alumina and 0.05 μm γ-alumina slurries, followed by thoroughly cleaning with ultra-pure Milli-Q water. The electrolyte solutions were deaerated by bubbling prepurified nitrogen gas for 8 min before measurements.

Reactive Oxygen Species (ROS) Generation Abilities

The total ROS generation abilities of the ligand (bpy-diRho)$(PF_6)_2$ and rhodium(III) complexes **1** – **4** were semi-quantitatively studied using DCFH-DA. The DCFH-DA stock solution in DMSO (500 μL, 1 mM) was added to NaOH aqueous solution (2 mL, 0.01 M) and kept in the dark at 298 K for 30 min to hydrolyse DCFH-DA into 2',7'-dichlorodihydrofluorescein (DCFH). Then, the mixture solution was diluted with PBS at pH 7.4 (10 mL) to prepare the final working solution. An aerated working solution containing DCFH (40 μM) and rhodium(III) complex (0.5 μM) was introduced to a quartz cuvette of 1-cm path length and irradiated with white light (400 – 700 nm, 2 mW cm^{-2}). The emission intensity at 525 nm was monitored within 10 min using an Edinburgh Instruments FS5 spectrofluorometer.

The superoxide anion ($O_2^{\bullet-}$) and hydroxyl ($HO^{\bullet}$) radicals generation abilities of the ligand (bpy-diRho)$(PF_6)_2$ and rhodium(III) complexes **1** – **4** were studied using DHR123 and HPF. An aerated working solution containing DHR123 (20 μM) or HPF (20 μM) and rhodium(III) complex (0.5 μM) was introduced to a quartz cuvette of 1-cm path length and irradiated with white light (400 – 700 nm, 2 mW cm^{-2}). The

emission intensity at 515 nm was monitored within 5 min using an Edinburgh Instruments FS5 spectrofluorometer.

Electron Paramagnetic Resonance (EPR) Measurements

The generation of $O_2^{\bullet-}$ and $HO^{\bullet}$ was investigated using DMPO as a spin-trapping agent. For the investigation of $O_2^{\bullet-}$, the sample solution containing DMPO (100 mM) and rhodium(III) complex (10 μM) was prepared in MeOH. For the investigation of $HO^{\bullet}$, the sample solution containing DMPO (100 mM) and rhodium(III) complex (10 μM) was prepared in PBS. After white-light irradiation (400 – 700 nm, 10 mW cm^{-2}) for 5 min, sample solutions were placed into glass capillary tubes with an internal diameter of 0.5 mm and sealed. The spectra were obtained on a Bruker EMXPlus-10/12 spectrometer at 298 K. EPR parameter settings were as follows: modulation amplitude 1 G, modulation frequency 100 kHz, microwave frequency 9.84 GHz and microwave power 20 mW. Each sample was scanned for 5 times.

Stability in Cell Culture Medium

Complex **2** (10 μM) was added to the growth medium/DMSO (99:1, *v*/*v*) and the mixture was incubated at 37°C for 24 h. After incubation, the solution was extracted with CH_2Cl_2 (1 mL × 3). The combined organic extract was dried over anhydrous $MgSO_4$ and filtered, and the solvent was removed under reduced pressure. The residual purple solid residue was dissolved in CH_3CN and analysed by ESI-MS.

Cellular Uptake Measurements

MCF-7 cells were grown in a 6-cm tissue culture dish in growth medium and incubated at 37°C under a 5% CO_2 atmosphere for 48 h. The medium was then removed and

replaced with the rhodium(III) complexes (10 μM) in growth medium/DMSO (99:1, *v*/*v*) at 37°C under a 5% CO_2 atmosphere for 6 h. The medium was removed and the cell layer was gently washed with PBS (1 mL × 3). The cells were trypsinised (0.5 mL) and harvested with PBS (0.5 mL). Cell numbers were obtained by a Logos Biosystem LUNA-II automated cell counter. The harvested cells were digested with 65% HNO_3 (0.5 mL) at 60°C for 1 h. The concentration of rhodium was determined by a NexION 2000 inductively coupled plasma-mass spectrometry (ICP-MS) (PerkinElmer SCIEX Instruments).

MTT Assays

MCF-7 cells were seeded in two 96-well flat-bottomed microplates in growth medium (100 μL) and grown at 37°C under a 5% CO_2 atmosphere for 48 h. The medium was then removed and the cells were treated with the rhodium(III) complexes with concentrations ranging from 50 to 0.01 μM in growth medium/DMSO (99:1, *v*/*v*). Wells containing untreated cells were used as a blank control. After incubation at 37°C under a 5% CO_2 atmosphere for 2 h, the medium in one of the microplates was replaced with phenol red-free growth medium and irradiated with white light (400 – 700 nm, 10 mW cm^{-2}) for 30 min. Then, the cells were incubated at 37°C under a 5% CO_2 atmosphere for 3.5 h. After incubation, the medium in each well of the two microplates was replaced with fresh growth medium (90 μL) and a solution of MTT in PBS (10 μL, 5 mg mL^{-1}). The medium was removed after incubation at 37°C under a 5% CO_2 atmosphere for 3 h and DMSO (200 μL) was then added to each well. The absorbance of the solutions at 570 nm was measured with a PerkinElmer EnSpire Microplate Reader. For the MTT assays performed under $CoCl_2$-induced hypoxic conditions, the cells were pretreated with $CoCl_2$ (150 μM) for 12 h prior to incubation with the

complexes, and $CoCl_2$ remained throughout the experiment. The subsequent procedures were the same as described above. For the photocytotoxicity study in the presence of various cell death inhibitors, the cells were pretreated with Fer-1 (ferroptosis inhibitor; 10 μM), z-VAD-fmk (apoptosis inhibitor; 25 μM), Nec-1 (necroptosis inhibitor; 50 μM) or NSA (pyroptosis inhibitor; 10 μM) for 12 h, followed by coincubation with complex **2** (1 μM) for 2 h and irradiation with white light (400 – 700 nm, 10 mW cm^{-2}) for 10 min, and subsequently incubated in the dark for 2 h.

Live-Cell Confocal Imaging

MCF-7 cells were seeded in a 2-cm confocal dish in growth medium and grown at 37°C under a 5% CO_2 atmosphere for 24 h. The medium was then removed and incubated with the ligand (bpy-diRho)$(PF_6)_2$ or rhodium(III) complexes (2 μM; λ_{ex} = 561 nm, λ_{em} = 575 – 650 nm) in growth medium/DMSO (99:1, *v*/*v*) at 37°C under a 5% CO_2 atmosphere for 30 min. After incubation, the medium was removed and the cell layer was washed gently with PBS (1 mL × 3). The cells were then incubated with MitoTracker Green (200 nM; λ_{ex} = 488 nm, λ_{em} = 500 – 530 nm) in growth medium at 37°C under a 5% CO_2 atmosphere for 15 min. After treatment, the medium was removed and the cell layer was gently washed with PBS (1 mL × 3). Laser-scanning confocal microscopy (LSCM) images were obtained using a Zeiss LSM 900 confocal microscope with a 63× oil-immersion objective lens. The Pearson's correlation coefficients (PCC's) were determined using the programme ImageJ (Version 1.53c).

Subcellular Distribution Analysis

MCF-7 cells were seeded in a 6-well plate in growth medium and grown at 37°C under a 5% CO_2 atmosphere for 48 h. The growth medium was then removed and replaced

with complex **2** (5 μM) in growth medium/DMSO (99:1, *v*/*v*) at 37°C under a 5% CO_2 atmosphere for 6 h. After treatment, the medium was removed and the cell layer was gently washed with PBS (1 mL × 3). The cells were trypsinised (0.5 mL) and harvested with PBS (0.5 mL). Cell numbers were obtained by a Logos Biosystem LUNA-II automated cell counter. Cellular fractionation was performed using a commercial kit (Abcam, Catalogue Number ab109719). All fractions were digested with 65% HNO_3 (0.5 mL) at 60°C for 1 h. The concentration of rhodium in each fraction was determined by ICP-MS.

Live/Dead Cell Staining Assays

MCF-7 cells were seeded in a 2-cm confocal dish in growth medium and grown at 37°C under a 5% CO_2 atmosphere for 24 h. The medium was then removed and the cells were incubated with complex **2** (2 μM) in growth medium/DMSO (99:1, *v*/*v*) at 37°C under a 5% CO_2 atmosphere for 2 h. After treatment, the medium was removed and the cell layer was gently washed with PBS (1 mL × 3). The cells were then replenished with phenol red-free growth medium and kept in the dark or irradiated at 525 nm (10 mW cm^{-2}) for 10 min. The medium was then replaced with fresh growth medium, and the cells were further incubated at 37°C under a 5% CO_2 atmosphere in the dark for 30 min before staining with Calcein-AM (1 μM; λ_{ex} = 488 nm, λ_{em} = 500 – 520 nm) and PI (10 μM; λ_{ex} = 532 nm, λ_{em} = 600 – 650 nm) for 1 h. After treatment, the medium was removed and the cell layer was gently washed with PBS (1 mL × 3). The cells were then imaged using a Leica TCS SPE confocal microscope with a 10× objective lens.

Monitoring of the Changes in Mitochondrial Membrane Potential (MMP)

MCF-7 cells were seeded in a 2-cm confocal dish in growth medium and grown at 37°C under a 5% CO_2 atmosphere for 24 h. The medium was then removed and the cells were incubated with complex **2** (2 μM) in growth medium/DMSO (99:1, *v*/*v*) at 37°C under a 5% CO_2 atmosphere for 2 h. After treatment, the medium was removed, and the cells were replenished with phenol red-free growth medium and irradiated with white light (400 – 700 nm, 10 mW cm^{-2}) for 10 min. The medium was then replaced with fresh growth medium, and the cells were incubated at 37°C under a 5% CO_2 atmosphere in the dark for 30 min before staining with R123 (5 μM; λ_{ex} = 488 nm, λ_{em} = 500 – 530 nm) for 10 min. The medium was then removed and the cell layer was gently washed with PBS (1 mL × 3). The cells were then imaged using a Zeiss LSM 900 confocal microscope and a 20× objective lens. Cells treated with complex **2** and R123 without light irradiation served as a control. For monitoring the changes in MMP under $CoCl_2$-induced hypoxic conditions, cells were pretreated with $CoCl_2$ (150 μM) for 12 h prior to incubation with the complex, and $CoCl_2$ remained throughout the experiment. The subsequent procedures were the same as described above.

Determination of Intracellular ROS

MCF-7 cells were seeded in a 2-cm confocal dish in growth medium and grown at 37°C under a 5% CO_2 atmosphere for 24 h. The intracellular ROS levels were measured using DCFH-DA, DHR123 or HPF to detect total ROS, $O_2^{\bullet-}$ and $HO^{\bullet}$, respectively. The cells were first treated with complex **2** (2 μM) in growth medium/DMSO (99:1, *v*/*v*) at 37°C under a 5% CO_2 atmosphere for 2 h and then incubated with DCFH-DA (5 μM, 30 min; λ_{ex} = 488 nm, λ_{em} = 500 – 530 nm), DHR123 (10 μM, 30 min; λ_{ex} = 488

nm, λ_{em} = 500 – 530 nm) or HPF (10 μM, 1 h; λ_{ex} = 488 nm, λ_{em} = 500 – 530 nm). After treatment, the medium was removed, and the cells were replenished with phenol red-free growth medium and irradiated with white light (400 – 700 nm, 10 mW cm^{-2}) for 5 min. The medium was then removed and the cell layer was gently washed with PBS (1 mL × 3). The cells were then imaged using a Zeiss LSM 900 confocal microscope with a 20× objective lens. Cells treated with complex **2** without light irradiation served as a control. For the intracellular ROS study performed under $CoCl_2$-induced hypoxic conditions, cells were pretreated with $CoCl_2$ (150 μM) for 12 h prior to incubation with the complex, and $CoCl_2$ remained throughout the experiment. The subsequent procedures were the same as described above.

LDH Release Assays

MCF-7 cells were seeded in two 96-well plates in growth medium and grown at 37°C under a 5% CO_2 atmosphere for 48 h. The medium was then removed and the cells were incubated with either fresh growth medium or complex **2** (5 μM) in growth medium/DMSO (99:1, *v*/*v*) at 37°C under a 5% CO_2 atmosphere for 2 h. After treatment, the medium was removed, and the cells were replenished with phenol red-free growth medium and kept in the dark or irradiated at 525 nm (10 mW cm^{-2}) for 10 min. The medium was then replaced with fresh growth medium, and the cells were incubated at 37°C under a 5% CO_2 atmosphere for 2 h. The supernatant of each well (50 μL) was collected and analysed using a commercial LDH cytotoxicity assay kit (Invitrogen, Catalogue Number C20300).

Immunofluorescence Staining

MCF-7 cells were seeded in two culture-insert 2-well confocal dishes in growth

medium and grown at 37°C under a 5% CO_2 atmosphere for 48 h. The medium was then removed and the cells were incubated with either fresh growth medium or complex **2** (5 μM) in growth medium/DMSO (99:1, *v*/*v*) at 37°C under a 5% CO_2 atmosphere for 2 h. After treatment, the medium was removed, and the cells were replenished with phenol red-free growth medium and kept in the dark or irradiated at 525 nm (10 mW cm^{-2}) for 10 min. The medium was then replaced with fresh growth medium, and the cells were incubated at 37°C under a 5% CO_2 atmosphere for 2 h. The medium was then removed, and the cell layer was gently washed with cold PBS (1 mL × 3). The cells were then fixed with paraformaldehyde (4%) in PBS for 10 min, permeabilised with Triton X-100 (0.1%) solution for 5 min and blocked with BSA (3%) for 1 h. The cells were then incubated with the primary antibody of caspase-1 (1:200) in PBS at 4°C overnight. After incubation, the cells were thoroughly washed with PBS (1 mL × 3) and further incubated with anti-rabbit Alexa Fluor 488-conjugated secondary antibody (1:1000; λ_{ex} = 488 nm, λ_{em} = 500 – 520 nm) in PBS at 37°C for 1 h. The cells were then washed with PBS (1 mL × 3) and the nuclei were stained with Hoechst 33258 (1 μg mL^{-1}; λ_{ex} = 405 nm, λ_{em} = 420 – 450 nm) for 10 min. After washing with PBS (1 mL × 3), the cells were imaged using a Leica TCS SPE confocal microscope with a 63× oil-immersion objective lens.

Western Blot Analysis

MCF-7 cells were seeded in two 24-well plates in growth medium and grown at 37°C under a 5% CO_2 atmosphere for 48 h. The medium was then removed and the cells were incubated with complex **2** (1 μM) in growth medium/DMSO (99:1, *v*/*v*) at 37°C under a 5% CO_2 atmosphere for 2 h. After treatment, the medium was removed, and the cells were replenished with phenol red-free growth medium and kept in the dark or

irradiated at 525 nm (10 mW cm^{-2}) for 5 min. The medium was then replaced with fresh growth medium, and the cells were incubated at 37°C under a 5% CO_2 atmosphere for 1 h. The cells were then washed with cold PBS (1 mL × 3), harvested and lysed using lysis buffer on ice. Following centrifugation for the collection of cellular lysates, the concentration of cellular protein was analysed by the BCA protein assay kit. Protein samples (25 μL/lane) were separated on an SDS-PAGE in a Tris-Glycine running buffer and blotted on polyvinylidene difluoride (PVDF) membranes. The PVDF membranes were then blocked with 5% BSA at room temperature for 1 h, followed by incubation with the primary antibody at 4°C overnight and the secondary antibody conjugated with horseradish peroxidase at room temperature for 1 h. Detection was performed by using the chemiluminescence (ECL) procedure. Equal loading of the proteins in each lane was verified by the intensity of β-actin and GAPDH.

Table S1. Crystallographic data of complex **1**.

Formula	$C_{95.67}H_{91.34}Cl_{7.34}F_{18}N_{10}O_2P_3Rh$
Formula weight	2210.94
Crystal system	triclinic
Space group (number)	P–1(2)
a/Å	17.8770(9)
b/Å	18.2248(9)
c/Å	18.6094(9)
α/°	90.143(2)
β/°	115.081(2)
γ/°	111.391(2)
Volume/Å^3	5023.5(4)
Z	2
ρ_{calc}/g cm^{-3}	1.462
μ/mm^{-1}	0.499
*F*000	2256
Crystal size/mm^3	0.40 × 0.36 × 0.35
Radiation	Mo *Kα* (λ = 0.71073 Å)
2θ range/°	4.41 to 55.19 (0.77 Å)
Index ranges	$-23 \le h \le 23$, $-23 \le k \le 23$, $-24 \le l \le 24$
Reflections collected	110505
Independent reflections	23231
Data/Restraints/Parameters	23231/14/1360
Goodness-of-fit on F^2	1.053

Final *R* indexes [$I \geq 2\sigma\ (I)$]	$R_1 = 0.0574$, w$R_2 = 0.1616$
Final *R* indexes [all data]	$R_1 = 0.0779$, w$R_2 = 0.1783$

Table S2. Selected bond lengths (Å) and angles (°) for complex **1**.

Rh(1)–N(1)	2.072(3)	Rh(1)–N(3)	2.078(3)
Rh(1)–N(5)	2.190(3)	Rh(1)–N(6)	2.246(3)
Rh(1)–C(1)	1.980(3)	Rh(1)–C(21)	1.997(4)
N(1)–Rh(1)–N(3)	171.0(2)	N(1)–Rh(1)–N(5)	108.1(6)
N(1)–Rh(1)–N(6)	87.8(4)	N(1)–Rh(1)–C(1)	80.3(4)
N(1)–Rh(1)–C(21)	92.3(7)	N(3)–Rh(1)–N(5)	77.9(8)
N(3)–Rh(1)–N(6)	100.2(9)	N(3)–Rh(1)–C(1)	94.2(5)
N(3)–Rh(1)–C(21)	80.0(1)	N(5)–Rh(1)–N(6)	74.2(2)
N(5)–Rh(1)–C(1)	169.8(7)	N(5)–Rh(1)–C(21)	99.2(5)
N(6)–Rh(1)–C(1)	101.4(5)	N(6)–Rh(1)–C(21)	173.1(5)
C(1)–Rh(1)–C(21)	85.6(3)		

Table S3. Electronic absorption spectral data of the ligand (bpy-diRho)$(PF_6)_2$ and rhodium(III) complexes **1** – **4** in CH_3CN at 298 K.

Compound	λ_{abs}/nm (ε/L mol^{-1} cm^{-1})
(bpy-diRho)$(PF_6)_2$	257 (57,560), 289 (46,750), 354 (15,910), 528 sh (68,380), 562 (170,470)
1	256 (81,390), 290 (61,310), 357 (32,725), 535 sh (59,585), 572 (137,555)
2	255 (90,660), 288 (65,825), 358 (30,230), 435 (13,410), 537 sh (58,810), 572 (132,500)
3	258 (104,985), 286 (91,910), 323 (70,100), 410 (27,670), 537 sh (59,415), 572 (128,725)
4	255 (108,015), 286 (83,175), 336 (56,790), 496 sh (26,895), 536 sh (68,024), 572 (130,545)

Table S4. Electrochemical data of free ligand (bpy-diRho)$(PF_6)_2$ and rhodium(III) complexes **1** – **4**.[a]

Compound	Oxidation, $E_{1/2}$/V	Reduction, $E_{1/2}$ or E_c/V
(bpy-diRho)$(PF_6)_2$	+1.25[b]	–0.71[c]
1	+1.26[b]	–0.61[b]
2	+1.25[b]	–0.61[b]
3	+1.25[b]	–0.61[b]
4	+1.25[b]	–0.62[b]

[a] In CH_3CN (0.1 M ^{n}BuNPF_6) at 298 K, glassy carbon electrode, sweep rate = 100 mV s^{-1}, all potentials are versus SCE.

[b] Quasi-reversible couples.

[c] Irreversible waves.

Table S5. Cellular uptake of complexes **1** – **4** in MCF-7 cells.

Complex	Amount of rhodium per MCF-7 cell/fmol[a]
1	0.22 ± 0.01
2	0.27 ± 0.01
3	0.15 ± 0.01
4	0.20 ± 0.01

[a] Amount of rhodium associated with an average MCF-7 cell upon incubation with the complexes (10 μM) at 37°C for 6 h, as determined by ICP-MS.

Fig. S1. Emission spectra of complexes **1** – **4** in EtOH/MeOH (4:1, *v*/*v*) at 77 K (λ_{ex} = 575 nm).

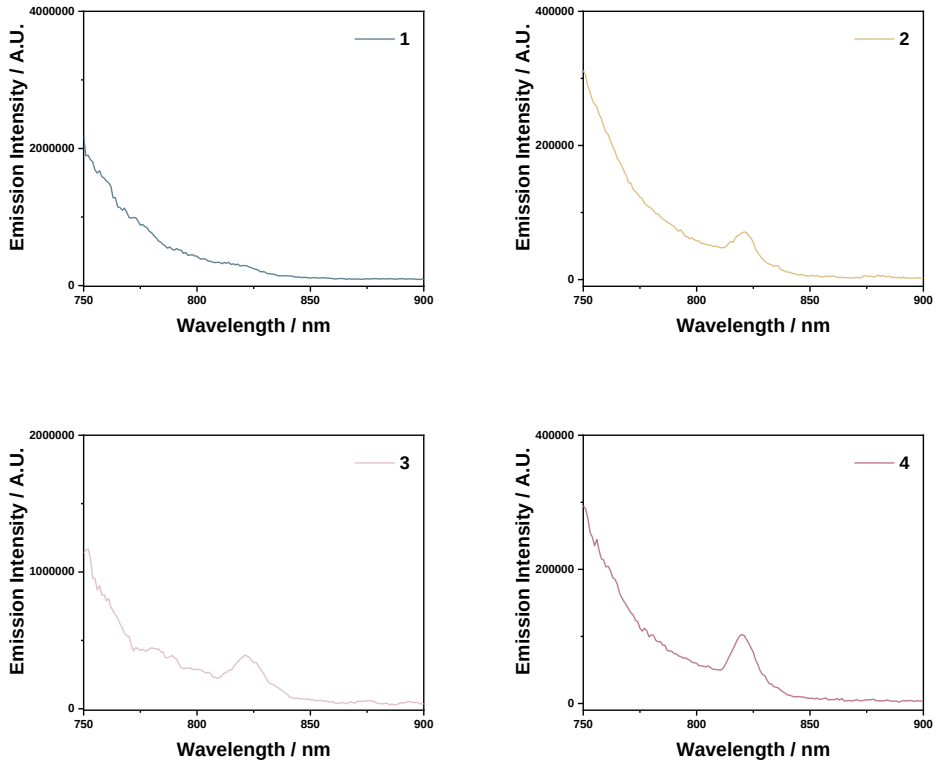

Fig. S2. Transient absorption difference spectra of the ligand (bpy-Rho)$(PF_6)_2$ and complex **1** in deaerated CH_3CN at 298 K (λ_{ex} = 532 nm).

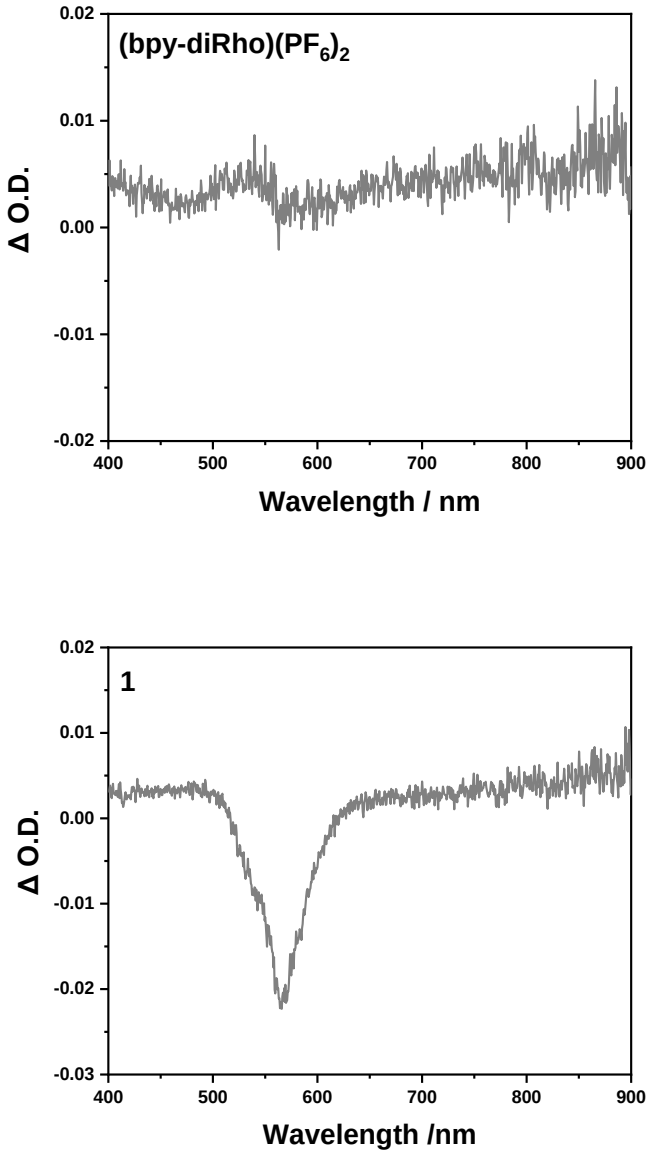

Fig. S3. Nanosecond time-resolved transient absorption difference spectra and the decay trace of the signal at 575 nm of complex **3** in deaerated CH_3CN at 298 K (λ_{ex} = 532 nm).

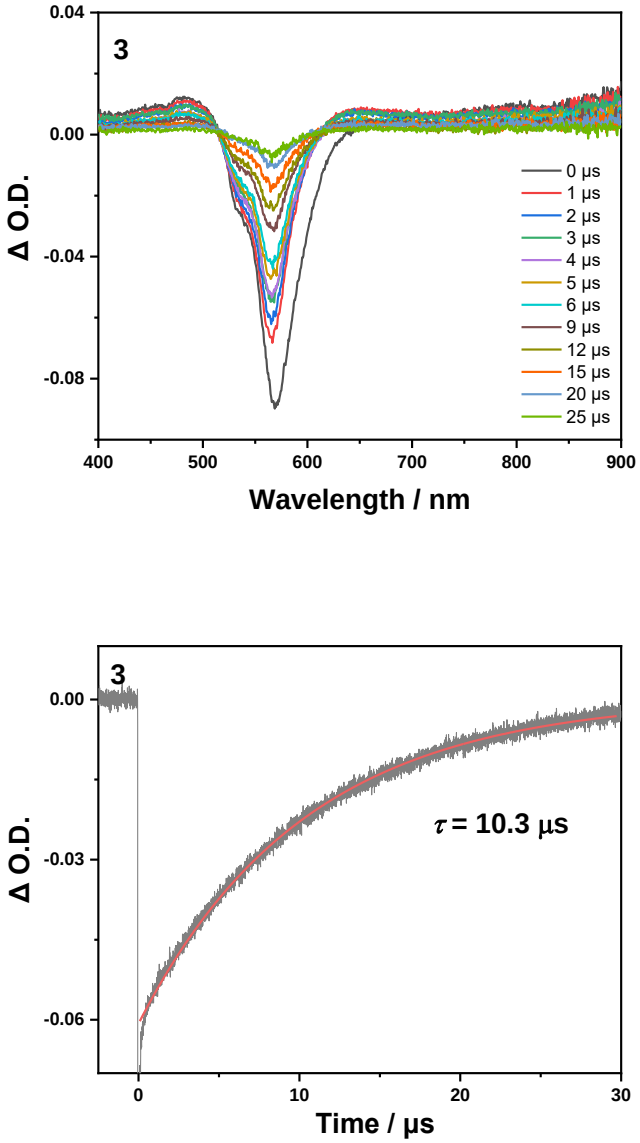

Fig. S4. Energy level diagram of dirhodamine-decorated rhodium(III) complexes.

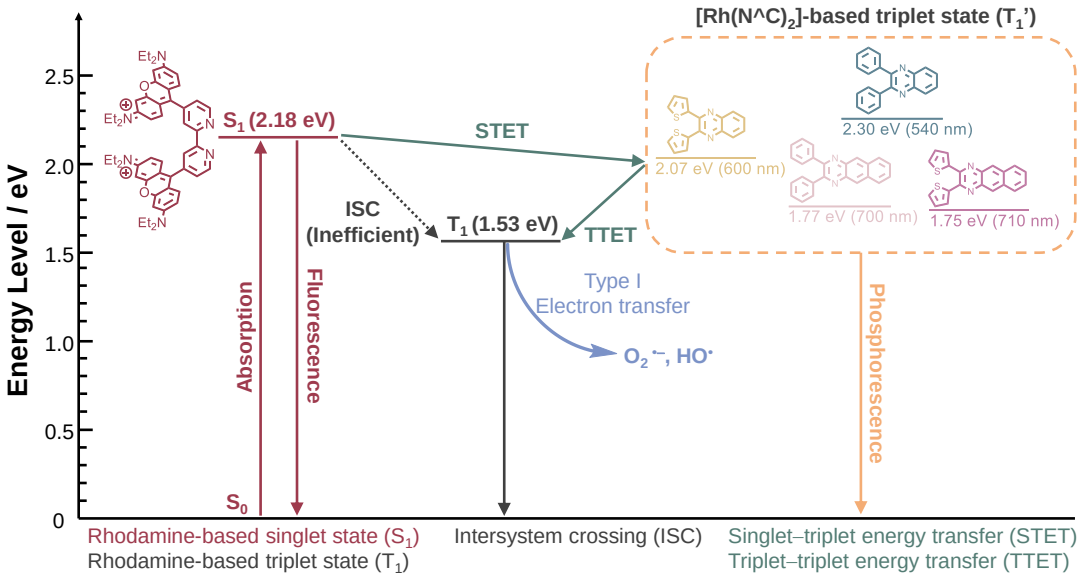

Fig. S5. Rates of decay of DPBF absorbance at 410 nm in aerated CH_3CN in the presence of complexes **1** – **4** and Rose Bengal upon photo irradiation (λ_{ex} = 570 nm).

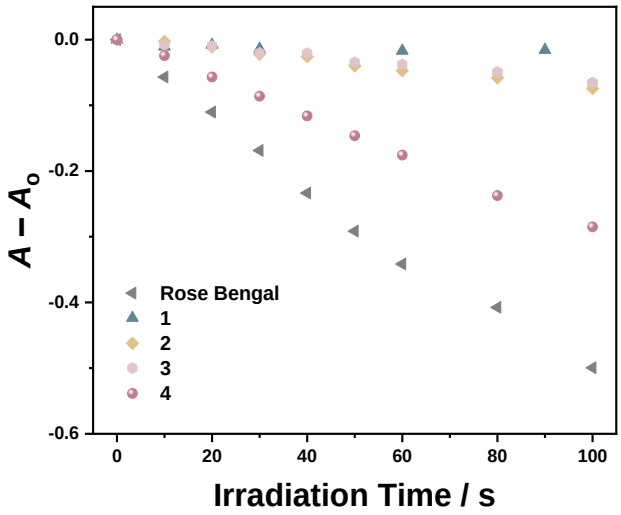

Fig. S6. Emission enhancement of an aerated PBS solution of DHR123 (20 μM; λ_{ex} = 488 nm) in the presence of complexes **2**, **2a** or **2b** (1 μM) at 515 nm upon photoirradiation (λ_{ex} = 570 nm).

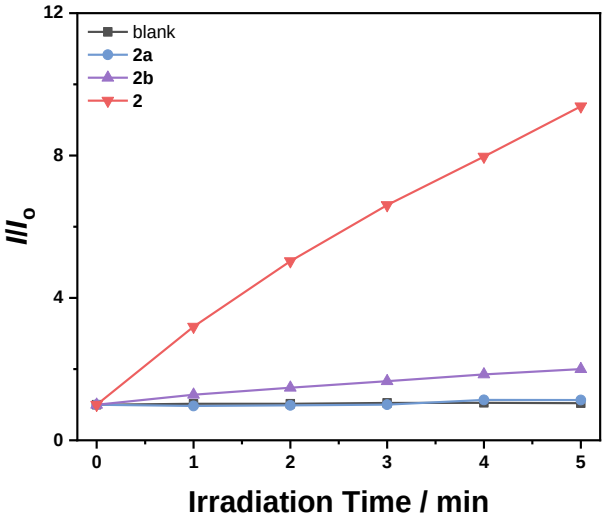

Fig. S7. Emission enhancement of an aerated PBS solution of HPF (20 μM; λ_{ex} = 488 nm) in the presence of complexes **2**, **2a** or **2b** (1 μM) at 515 nm upon photoirradiation (λ_{ex} = 570 nm).

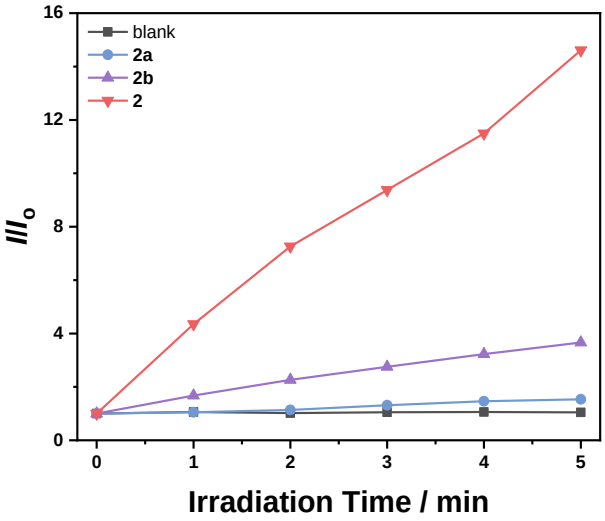

Fig. S8. Cyclic voltammograms of (bpy-diRho)$(PF_6)_2$ and complexes **1** – **4** in deaerated CH_3CN at 298 K versus SCE (0.1 M $^nBu_4NPF_6$).

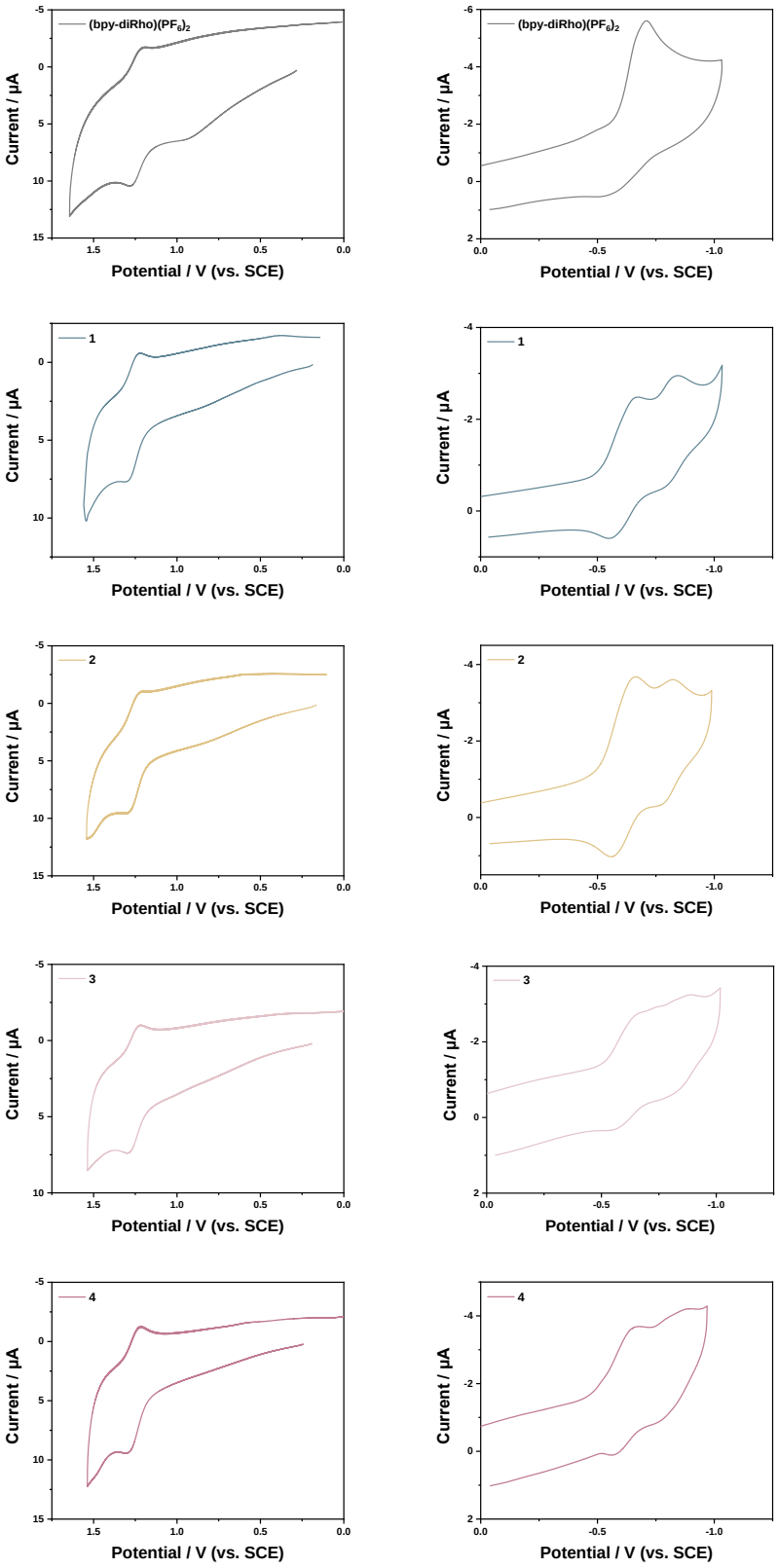

Fig. S9. Latimer diagrams showing the excited-state redox potentials of complexes **1** – **4** *versus* SCE.

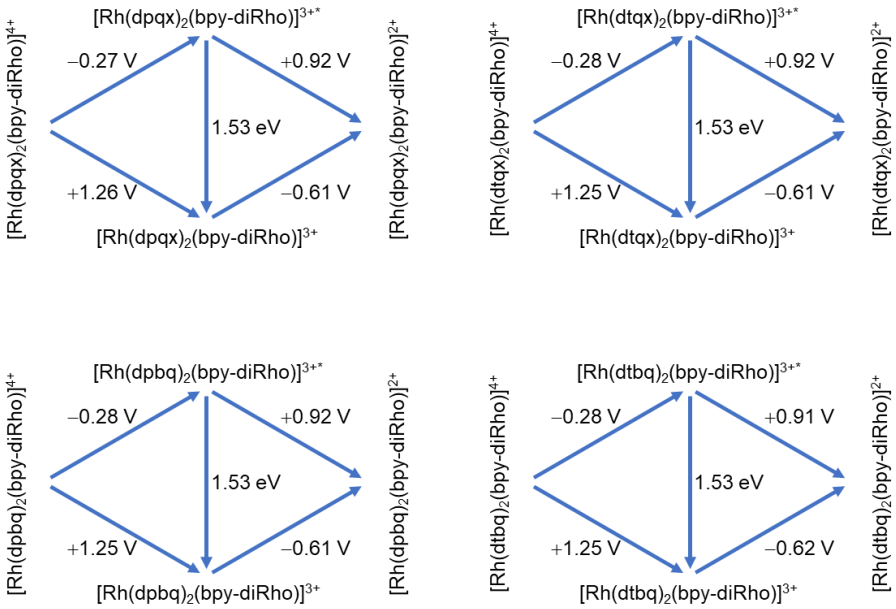

Fig. S10. ESI-mass spectrum of a CH_2Cl_2 extract of complex **2** (10 μM) incubated in DMEM at 37°C for 24 h.

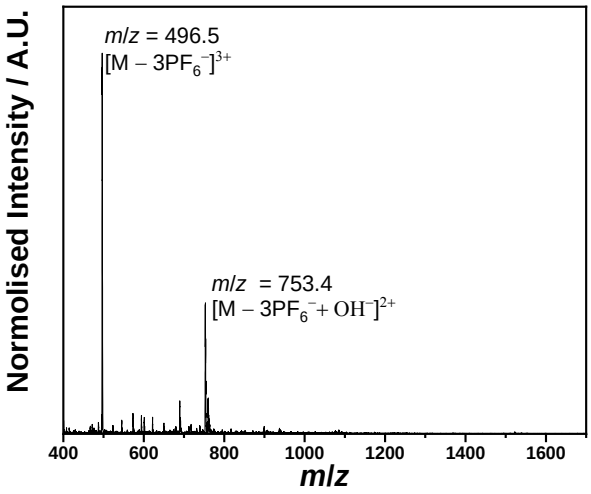

Fig. S11. LSCM images of live MCF-7 cells incubated with (bpy-diRho)$(PF_6)_2$ or complexes **1**, **3** and **4** (5 μM, 30 min; λ_{ex} = 561 nm, λ_{em} = 575 – 650 nm) and then with MitoTracker Green (200 nM, 15 min; λ_{ex} = 488 nm, λ_{em} = 500 – 525 nm).

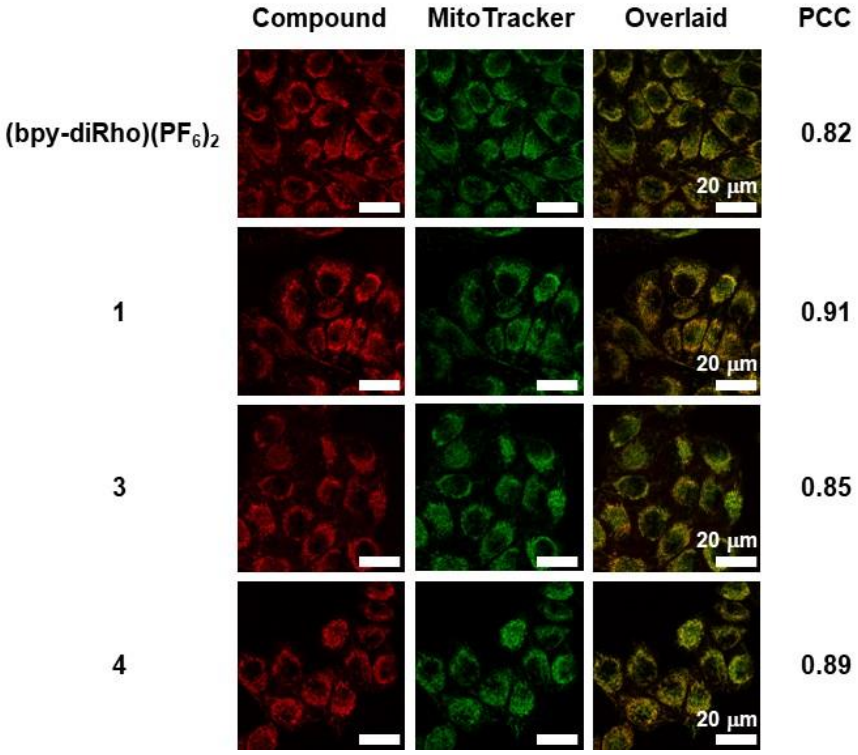

Fig. S12. Subcellular distribution of complex **2** in MCF-7 cells. The cells were incubated with complex **2** (5 μM) for 6 h and then fractionated into mitochondria, nucleus and cytosol using a commercial kit. The rhodium content in each fraction was determined by ICP-MS.

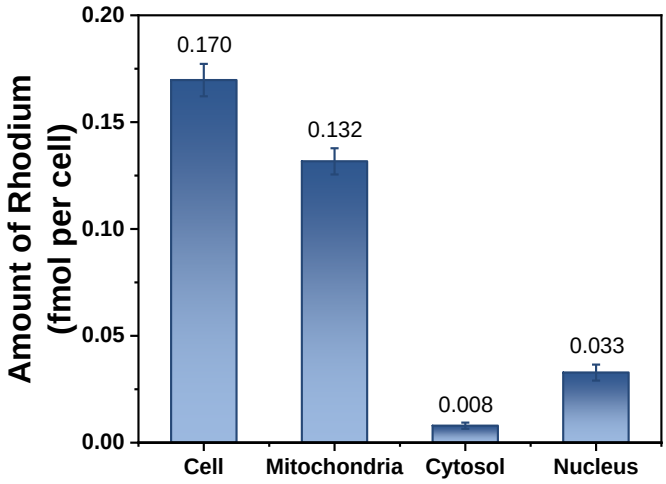

Fig. S13. Cytotoxicity of complexes **1** – **4** towards MCF-7 cells upon incubation in the dark for 6 h under normoxic conditions.

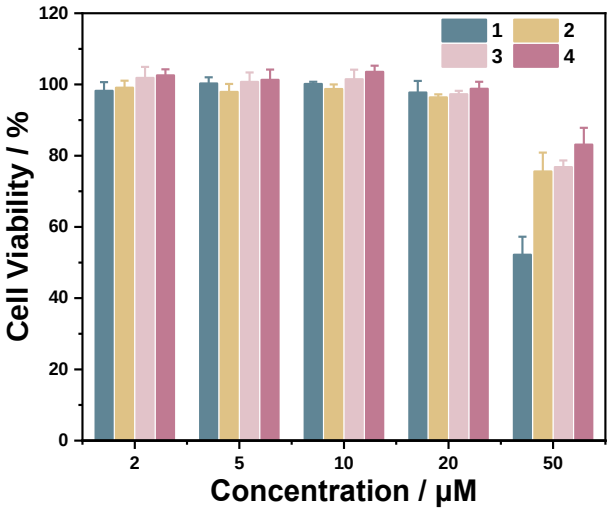

Fig. S14. Photocytotoxicity of complexes **1** – **4** towards MCF-7 cells under normoxic conditions. The cells were incubated with the complexes for 2 h, followed by irradiation with white light (400 – 700 nm, 10 mW cm^{-2}) for 30 min, and subsequently incubated in the dark for 3.5 h.

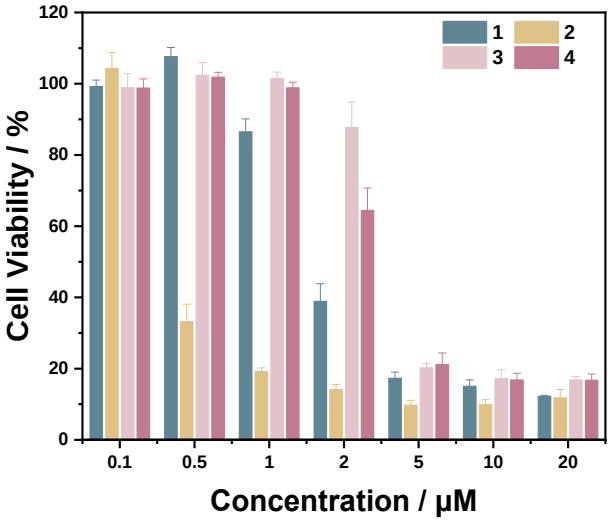

Fig. S15. Cytotoxicity of complexes **1** – **4** towards MCF-7 cells upon incubation in the dark for 6 h under $CoCl_2$-induced hypoxic conditions.

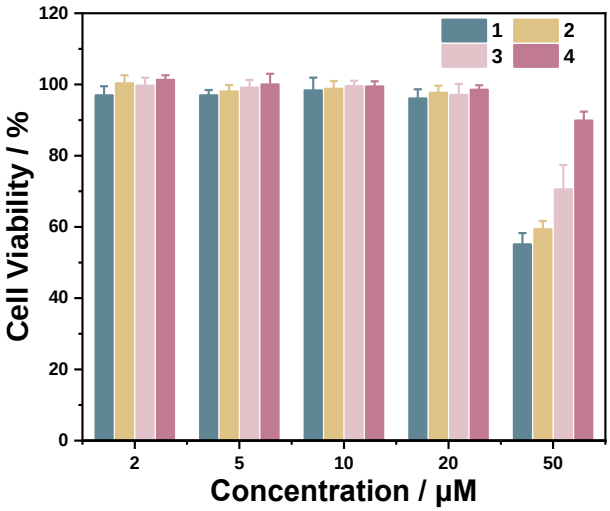

Fig. S16. Photocytotoxicity of complexes **1** – **4** towards MCF-7 cells under $CoCl_2$-induced hypoxic conditions. The cells were pretreated with $CoCl_2$ (150 μM) for 12 h and then incubated with the complexes for 2 h, followed by irradiation with white light (400 – 700 nm, 10 mW cm^{-2}) for 30 min, and subsequently incubated in the dark for 3.5 h.

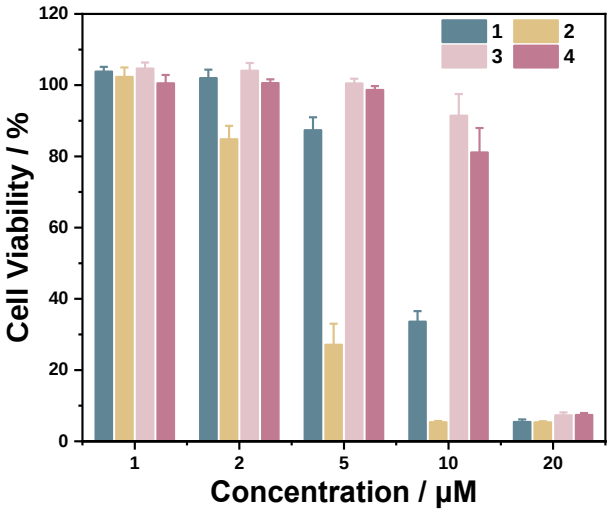

Fig. S17. Changes in MMP in complex **2**-treated MCF-7 cells upon light irradiation under $CoCl_2$-induced hypoxic conditions. The cells were pretreated with $CoCl_2$ (150 μM, 12 h) and then incubated with complex **2** (2 μM, 2 h). The cells were subsequently incubated in the dark or irradiated with white light (400 – 700 nm, 10 mW cm^{-2}) for 10 min, followed by incubation in the dark for 30 min and staining with R123 (5 μM, 10 min; λ_{ex} = 488 nm, λ_{em} = 500 – 530 nm) prior to imaging experiments.

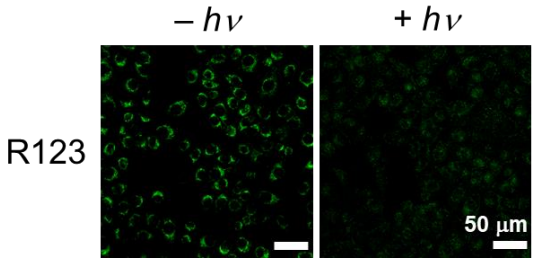

Fig. S18. Mitochondrial ROS generation in complex **2**-treated MCF-7 cells upon light irradiation. The cells were incubated with complex **2** (2 μM, 2 h) and then with DHR123 (10 μM, 30 min; λ_{ex} = 488 nm, λ_{em} = 500 – 530 nm). The cells were subsequently incubated in the dark or irradiated with white light (400 – 700 nm, 10 mW cm^{-2}) for 5 min, followed by staining with MitoTracker Deep Red (200 nM, 15 min; λ_{ex} = 635 nm, λ_{em} = 650 – 700 nm) prior to imaging experiments.

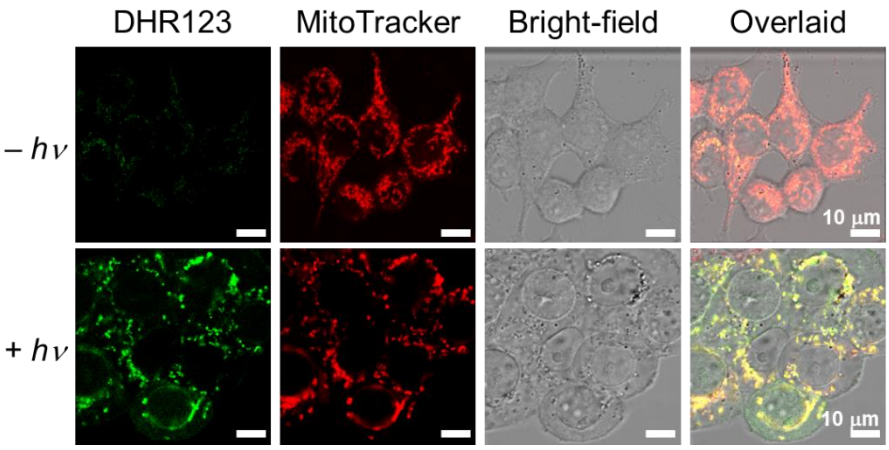

Fig. S19. Intracellular ROS generation in complex **2**-treated MCF-7 cells upon light irradiation under $CoCl_2$-induced hypoxic conditions. The cells were pretreated with $CoCl_2$ (150 μM, 12 h) and incubated with complex **2** (2 μM, 2 h). The cells were then stained with DCFH-DA (5 μM, 30 min; λ_{ex} = 488 nm, λ_{em} = 500 – 530 nm), DHR123 (10 μM, 30 min; λ_{ex} = 488 nm, λ_{em} = 500 – 530 nm) or HPF (10 μM, 1 h; λ_{ex} = 488 nm, λ_{em} = 500 – 550 nm), followed by incubation in the dark or irradiation with white light (400 – 700 nm, 10 mW cm^{-2}, 5 min) prior to imaging experiments.

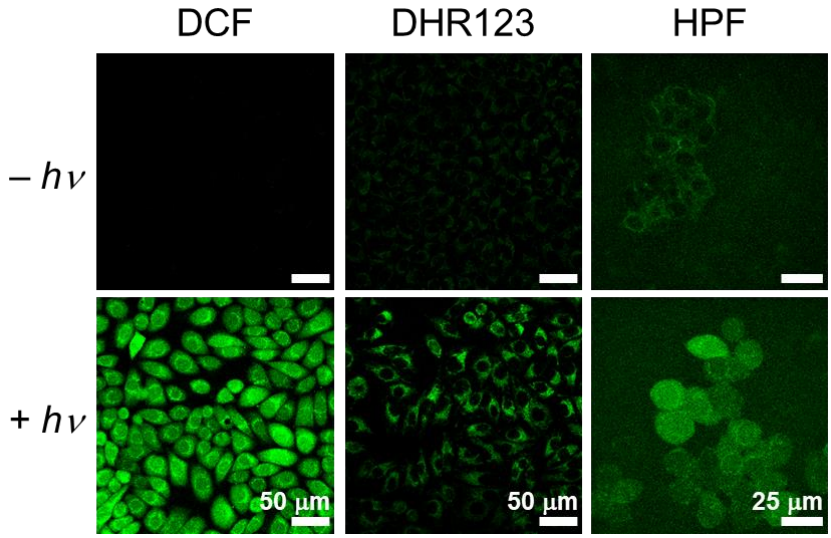

Fig. S20. Viability of complex **2**-treated MCF-7 cells with or without pretreatment of pathway-specific inhibitors to assess the mechanism of photoinduced cell death. The cells were pretreated with Fer-1 (ferroptosis inhibitor; 10 μM), z-VAD-fmk (apoptosis inhibitor; 25 μM), Nec-1 (necroptosis inhibitor; 50 μM) or NSA (pyroptosis inhibitor; 10 μM) for 12 h, followed by coincubation with complex **2** (1 μM) for 2 h, irradiation with white light (400 – 700 nm, 10 mW cm^{-2}) for 10 min and a subsequent incubation in the dark for 2 h.

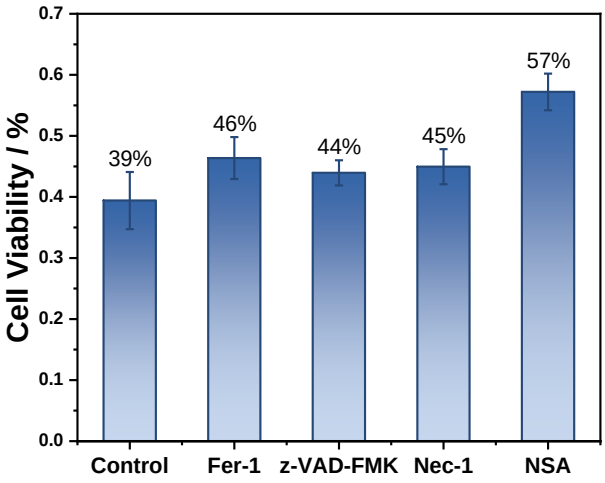

Fig. S21. ^{1}H NMR spectrum of (bpy-diRho)$(PF_6)_2$ in CD_3CN at 298 K.

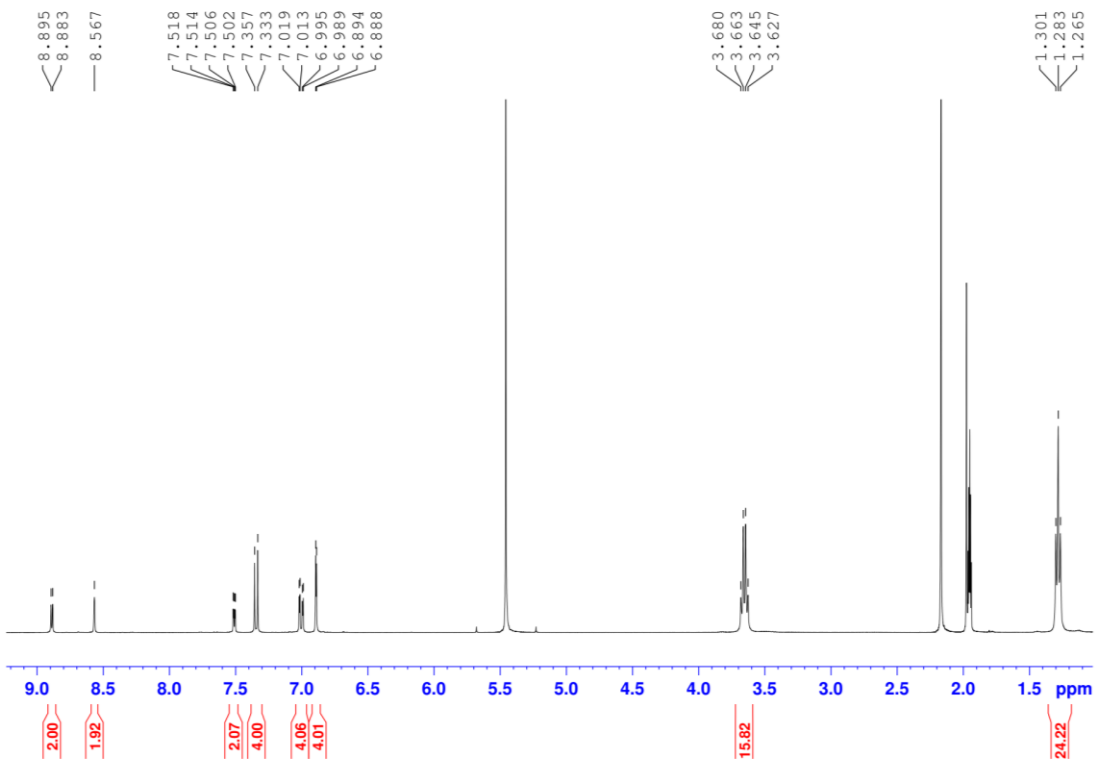

Fig. S22. ^{13}C NMR spectrum of (bpy-diRho)$(PF_6)_2$ in CD_3CN at 298 K.

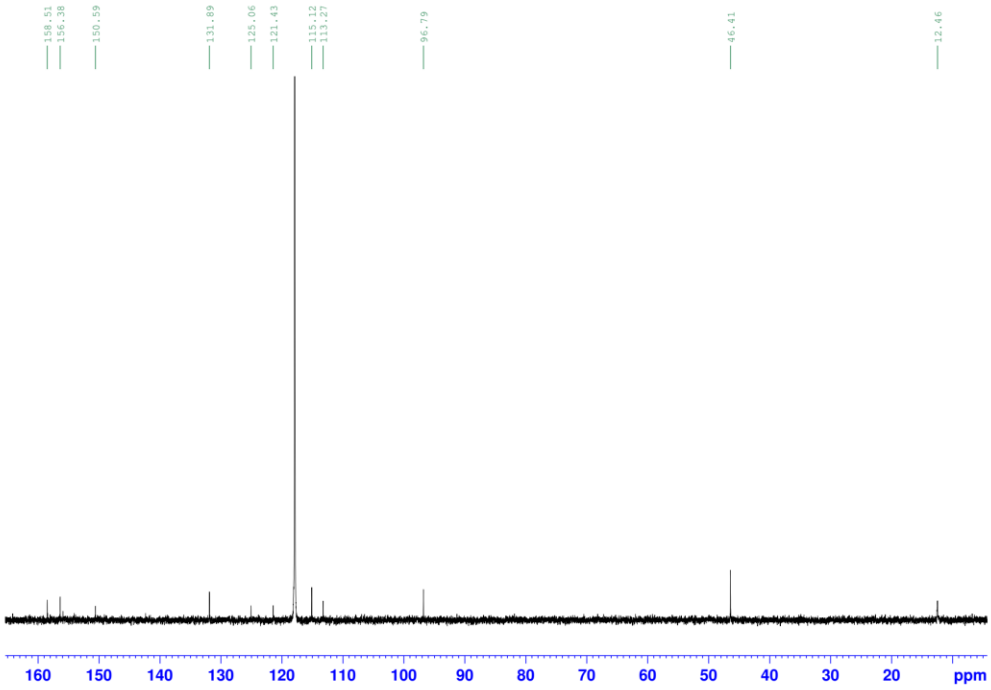

Fig. S23. ^{1}H NMR spectrum of complex **1** in CD_3CN at 298 K.

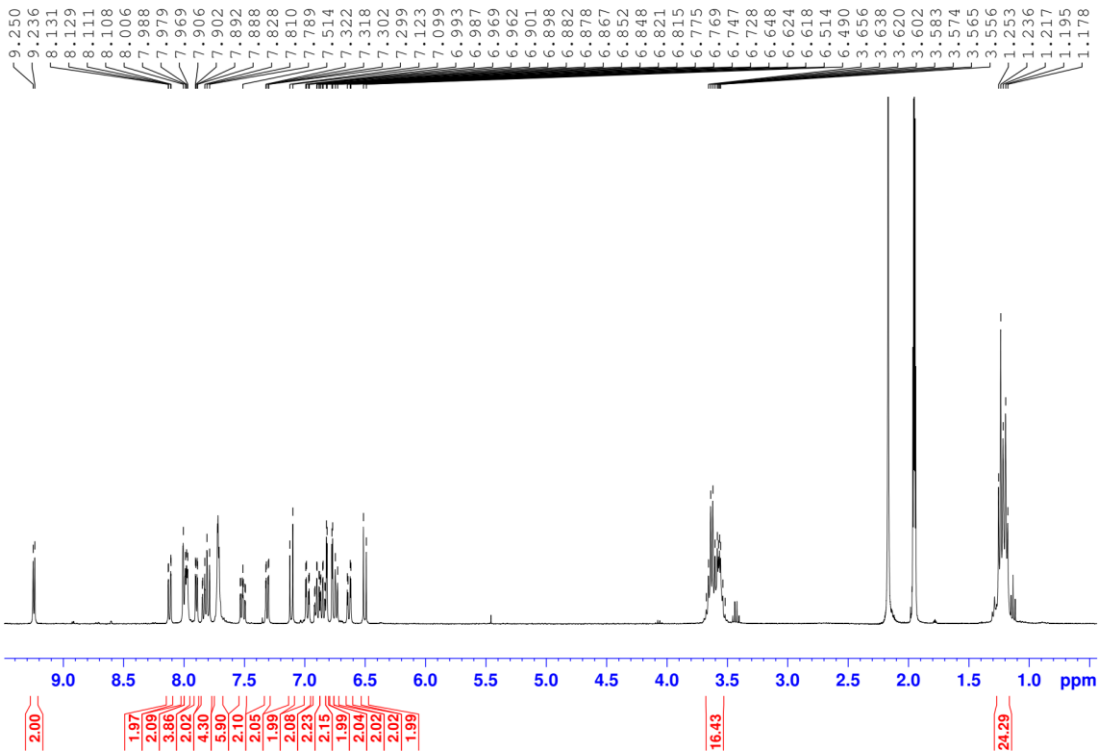

Fig. S24. ^{13}C NMR spectrum of complex **1** in CD_3CN at 298 K.

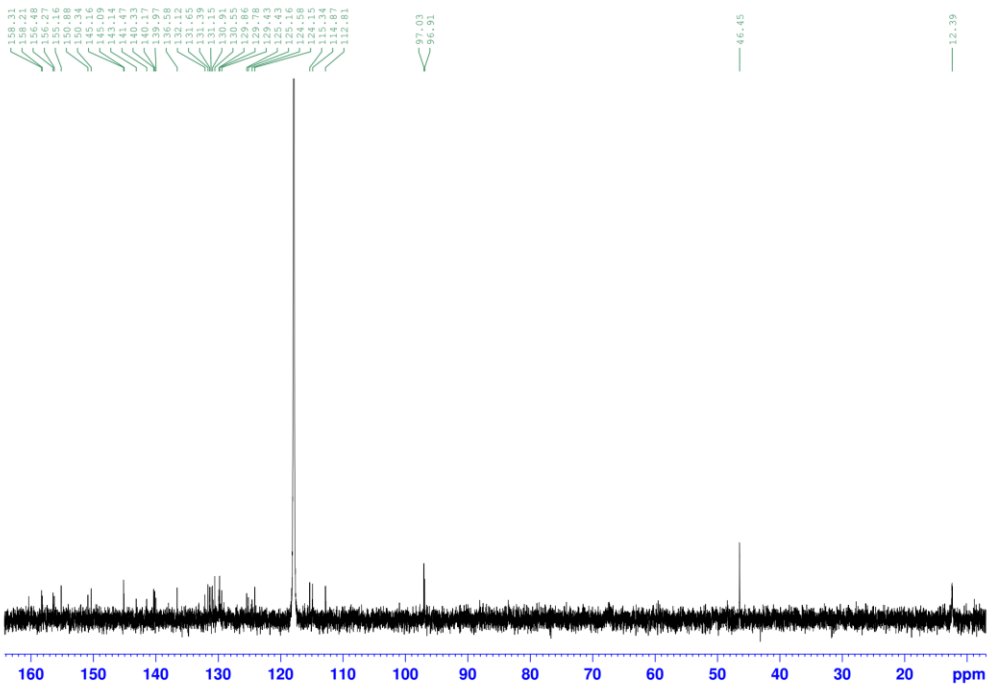

Fig. S25. ^{1}H NMR spectrum of complex **2** in CD_3CN at 298 K.

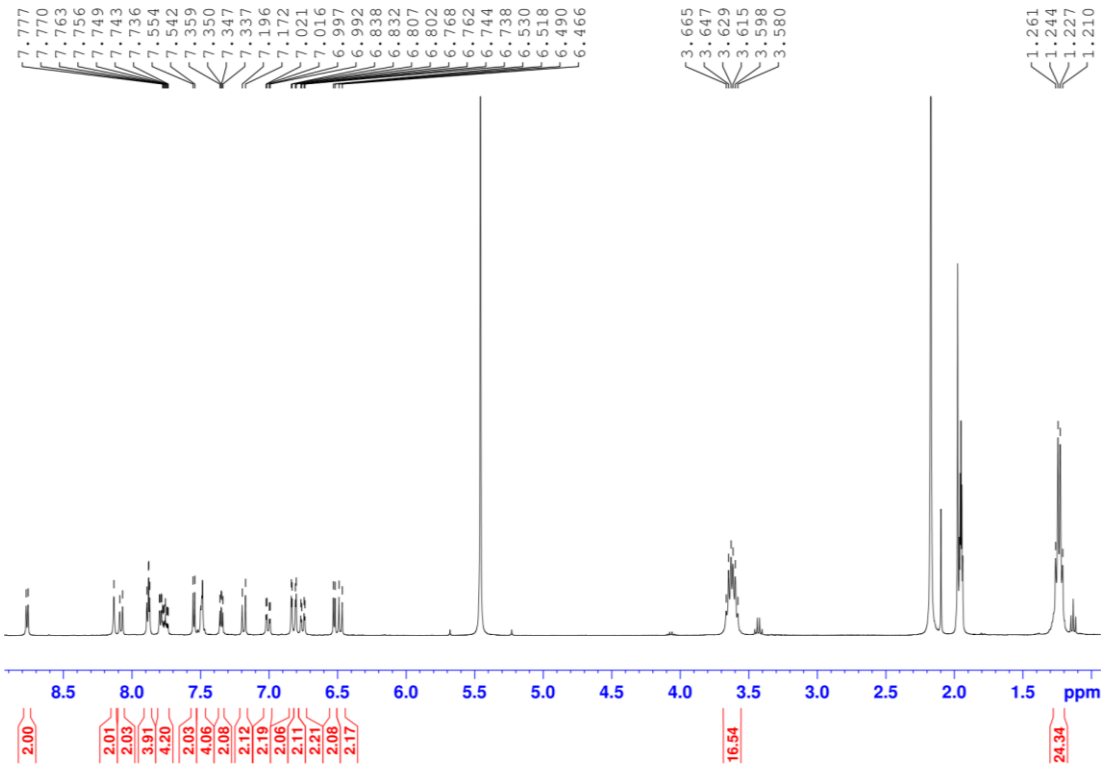

Fig. S26. ^{13}C NMR spectrum of complex **2** in CD_3CN at 298 K.

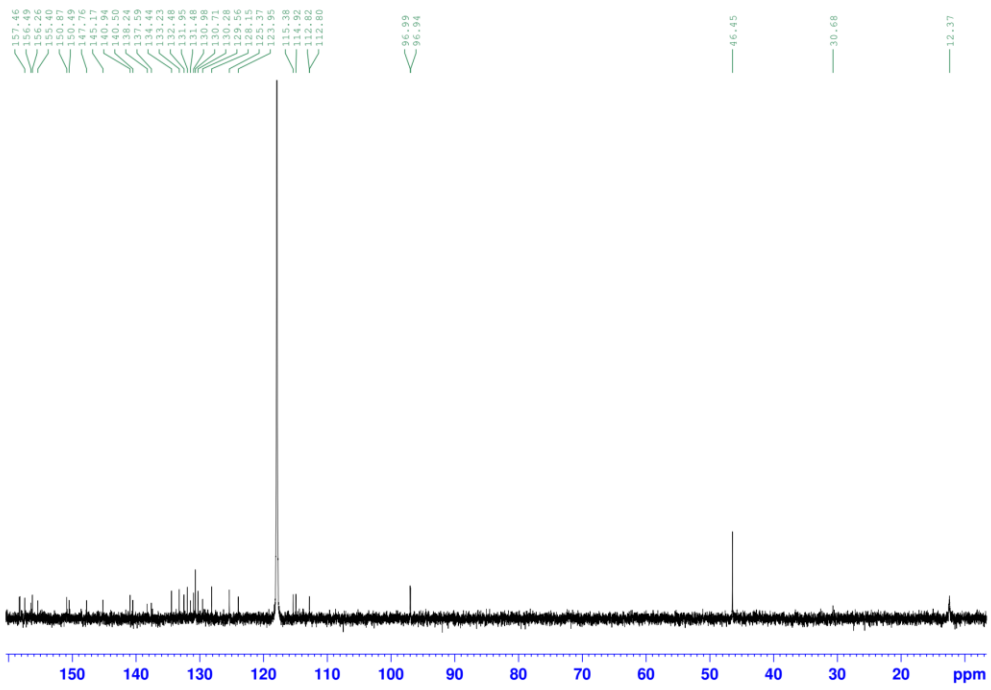

Fig. S27. ^{1}H NMR spectrum of complex **3** in CD_3CN at 298 K.

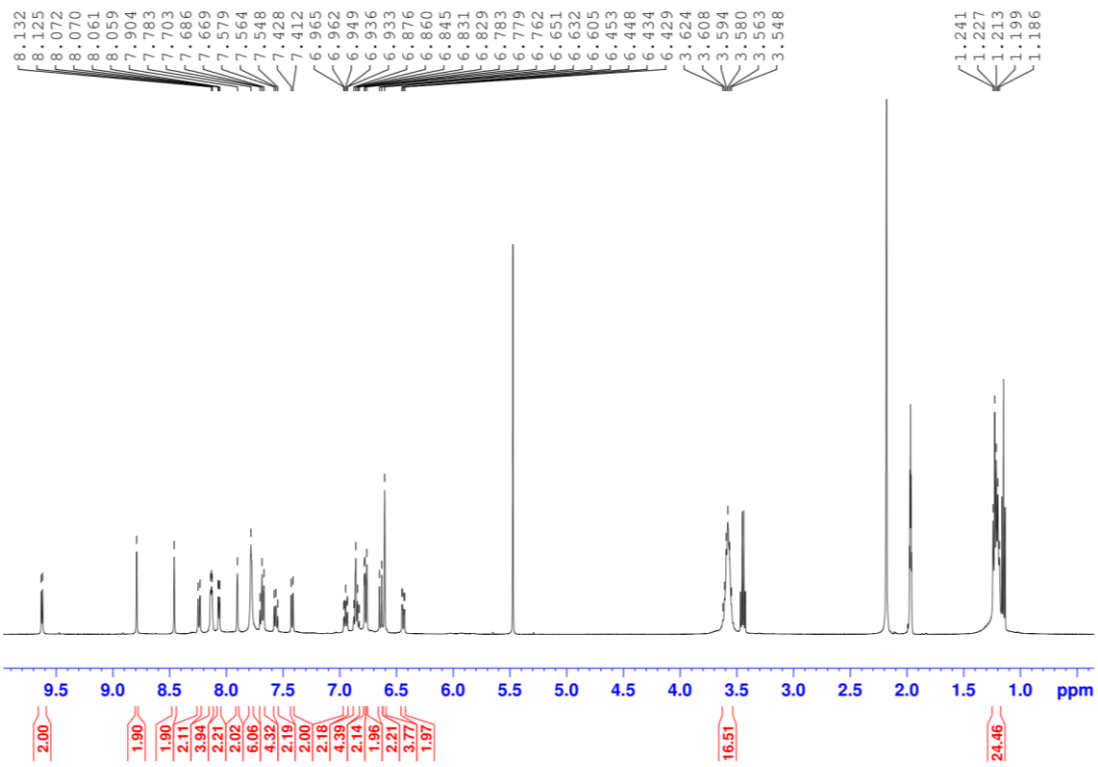

Fig. S28. ^{13}C NMR spectrum of complex **3** in CD_3CN at 298 K.

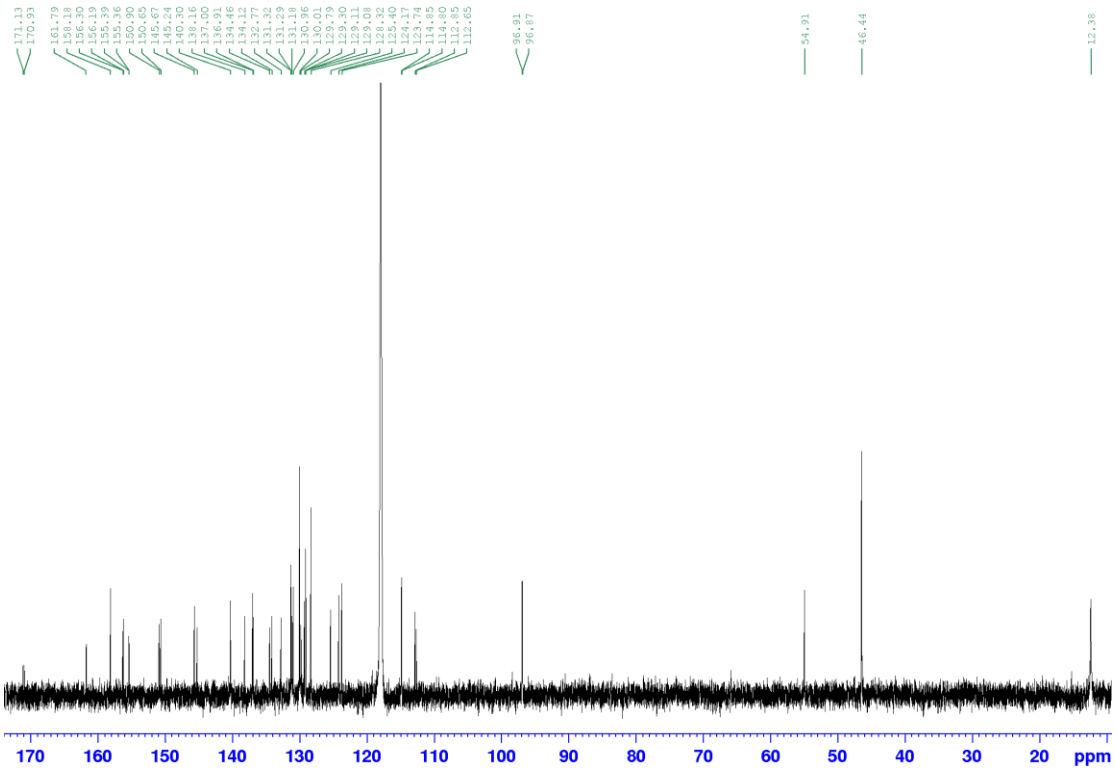

Fig. S29. ^{1}H NMR spectrum of complex **4** in CD_3CN at 298 K.

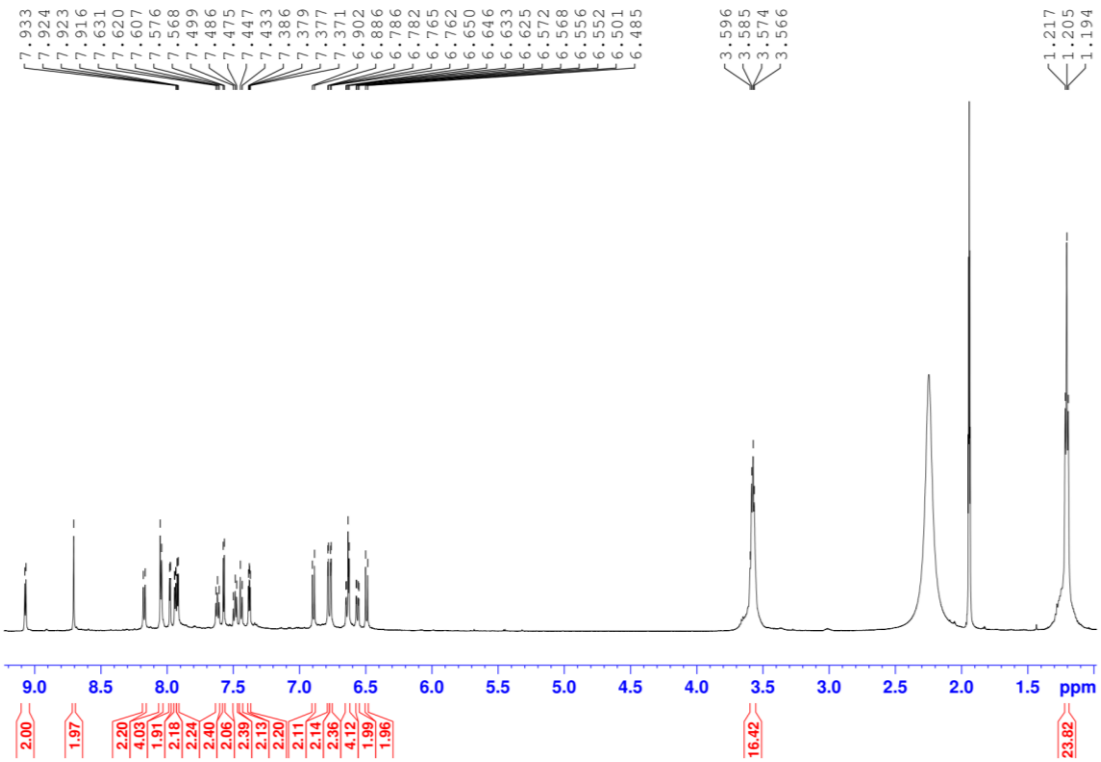

Fig. S30. ^{13}C NMR spectrum of complex **4** in CD_3CN at 298 K.

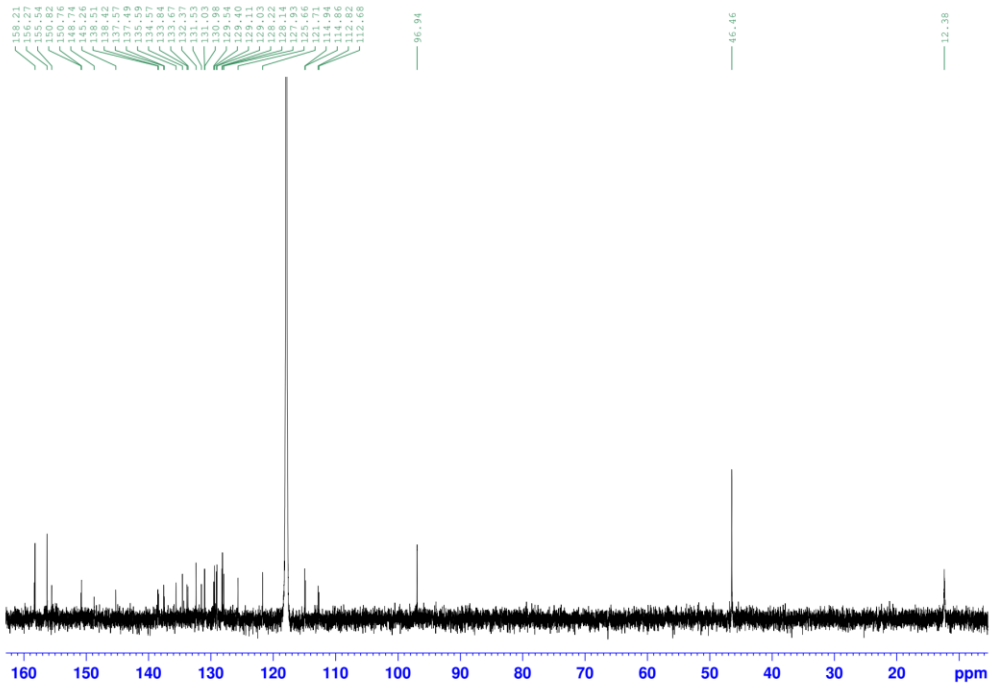

References

[1] W. L. F. Armarego, *Purification of Laboratory Chemicals*, 8th ed, Butterworth Heinemann, Oxford, **2017**.

[2] H. Oh, J. Kim, S. H. Yun, J. Lee, B. Park, J. Tak and B. H. Kim, *Synth. Met.*, **2014**, *198*, 260.

[3] F. R. Díaz, M. A. del Valle, C. Núñez, A. Godoy, J. L. Mondaca, A. Toro-Labbé and J. C. Bernède, *Polym. Bull.*, **2006**, *56*, 155.

[4] F. Wei, S.-L. Lai, S. Zhao, M. Ng, M.-Y. Chan, V. W.-W. Yam and K. M.-C. Wong, *J. Am. Chem. Soc.*, **2019**, *141*, 12863.

[5] G. A. Crosby and J. N. Demas, *J. Phys. Chem.*, **1971**, *75*, 991.

[6] F. Stracke, M. Heupel and E. Thiel, *J. Photochem. Photobiol. A Chem.*, **1999**, *126*, 51.